Terrestrial Rock Coatings[☆]

Ronald I Dorn, School of Geographical Sciences & Urban Planning, Arizona State University, Tempe, AZ, United States

1 Introduction to terrestrial rock coatings

Bare rock surfaces rarely display a rock's true appearance, where rhyolite appears pink, gneiss displays dark and light banding or basalt is black. As surfaces accrete rock coatings (Table 1) can dramatically "paint a landscape"—as exemplified by Yosemite Valley, United States (Larson and Dorn, 2012) and the granite rock walls in the Mont Blanc massif, western European Alps (Gallach et al., 2021). Consider three examples in Fig. 1. The sandstone of Petra, Jordan, is often darkened by case hardening caused by the accumulation of iron and manganese in the upper millimeter of sandstone (upper row in Fig. 1). The light colored granitic dome at Stone Mountain, Georgia, is streaked by several different types of rock coatings, including calcium oxalate (middle row in Fig. 1). Black basalt lava flows on the rainshadow side of Hualalai and Mauna Loa volcanoes, Hawaii, are gradually lightened in color as silica glaze accrete on lava flow surfaces (lower row in Fig. 1). The geomorphic reality is that coated surfaces are far more common than uncoated rocks. Because these accretions influence the rock decay of the underlying rock, a full understanding of the terrestrial weathering environment must consider rock coatings.

This article organizes rock coatings through the lens of the paradigm of landscape geochemistry, as developed by Soviet geography (Polynov, 1937; Perel'man, 1961, 1966; Glazovskaya, 1968, 1973) with some adoption outside of Russia (Fortescue, 1980). This well-established theoretical framework provides a way to interpret rock coatings in terms of element abundance, element migration, geochemical flows, geochemical gradients, and geochemical barriers with the classification, interpretation, and spatial laws pertaining to geochemical landscapes. At its simplest, a landscape geochemical approach interprets the occurrence of rock coatings as being caused by physical, chemical or biological barriers to the transport of elements. This article analyzes rock coatings from the perspective of five different landscape geochemistry hierarchies of controls on rock coating formation.

2 Interpreting terrestrial rock coatings through a landscape geochemistry approach

What influences the formation of a rock coating? Phased more empirically, the issue involves the processes that generate silica glaze on one surface, case hardening on another, and oxalate crusts on a third—as exemplified by the three different types of rock coatings seen in Fig. 1.The answer in the literature typically ends up being an encyclopedic approach of analyzing unique site-specific factors. For the case hardening at Petra (upper row in Fig. 1), rock varnish once formed on a sandstone surface. Manganese and iron leached out of the overlying varnish coating reprecipitates inside the pore spaces of the sandstone. Granular disintegration of the sandstone surface keeps varnish thickness to a few micrometers, but case hardening by these heavy metals stabilizes the outer millimeter of weathering rind.

Another coating is the oxalate crust on Stone Mountain, Georgia (middle row in Fig. 1); this oxalate, composed primary of hydrated calcium oxalate ($CaC_2O_4 \cdot H_2O$), accreted about a meter downslope from a patch of lichens. Overland flow carried oxalate from the lichens, and evaporation assisted in the accretion of the oxalate crust.

Silica glaze formed on the 1859 Mauna Loa lava flow (lower row in Fig. 1) started with soluble Al-Si complexes [$Al(OSi(OH)^3)^{2+}$] that are ubiquitous on silicate mineral surfaces. Gentle wetting from dew or even water vapor is enough to mobilize these Al-Si complexes. There is a transition between complete and partial wetting; this transition rests at about 20–70 nm. When this transition is crossed, the metastable wetting film on the silica surface ruptures and silica precipitates (Langworthy et al., 2010).

These empirical examples exemplify the norm in the rock-coating literature: general lack of theory in rock coating research. In fact, the only theory yet proposed to explain the occurrence of different types of rock coatings (Table 1) is landscape geochemistry.

[☆]*Change History*: August 2021. RI Dorn updated the 2011 version with new references, additions and deletions in some sections, and new illustrations (Figures 4, 25, 32, 34, and 36).

Table 1   Major types of rock coatings.

Coating	Description	Related terms
Carbonate Skin	Composed primarily of carbonate, usually $CaCO_3$, but sometimes $MgCO_3$	Calcrete, travertine
Case Hardening	Addition of cementing agent to rock matrix material; the agent may be manganese, sulfate, carbonate, silica, iron, oxalate, organisms, or anthropogenic.	Sometimes called a particular type of rock coating
Dust Film	Light powder of clay- and silt-sized particles attached to rough surfaces and in rock fractures.	Clay skins; clay films; soiling
Heavy Metal Skins	Coatings of iron, manganese, copper, zinc, nickel, mercury, lead and other heavy metals on rocks in natural and human-altered settings.	Also described by chemical composition
Iron Film	Composed primarily of iron oxides or oxyhydroxides	Ferric oxide, iron staining
Lithobiontic Coatings	Organisms forming rock coatings, for example lichens, moss, fungi, cyanobacteria, algae.	Organic mat, biofilms, biotic crust
Nitrate Crust	Potassium and calcium nitrate coatings on rocks, often in caves and rock shelters in limestone areas.	Saltpeter; niter; icing
Oxalate Crust	Mostly calcium oxalate and silica with variable concentrations of magnesium, aluminum, potassium, phosphorus, sulfur, barium, and manganese. Often found forming near or with lichens.	Oxalate patina, lichen-produced crusts, patina, scialbatura
Phosphate Skin	Various phosphate minerals (e.g., iron phosphates or apatite) sometimes mixed with clays and sometimes manganese.	Organophosphate film; epilithic biofilm
Pigment	Human-manufactured material placed on rock surfaces by people.	Pictograph, paint, graffiti
Rock Varnish	Clay minerals, Mn and Fe oxides, and minor and trace elements; color ranges from orange to black in color produced by variable concentrations of different manganese and iron oxides.	Desert varnish, patina, Wüstenlack
Salt Crust	Chloride precipitates formed on rock surfaces	Halite crust, efflorescence
Silica Glaze	Usually clear white to orange shiny lustre, but can be darker in appearance, composed primarily of amorphous silica and aluminum, but often with iron.	Desert glaze, turtle-skin patina, siliceous crusts, silica-alumina coating, silica skins
Sulfate Crust	Sulfates (e.g., barite, gypsum) on rocks; not gypsum crusts that are sedimentary deposits	Sulfate skin

Dorn RI (1998) *Rock Coatings.* Elsevier: Amsterdam, 429 pp.

Because the science of "weathering" (better termed "rock decay" (Hall et al., 2012)) in geomorphology is a search for broader explanatory patterns, case studies do not advance the development of general theory. The exception is the field of landscape geochemistry (Polynov, 1937; Perel'man, 1961, 1966; Glazovskaya, 1968, 1973) that offers a systematic way of analyzing the geography rock coatings. Using this spatial approach to understanding biogeochemistry, Dorn (1998) proposed five general hierarchies of controls on the development of rock coatings. Although I advocate landscape geochemistry as theoretical frmework to understand spatial patterns of rock coatings, a dialogue on development of alternative theoretical frameworks for rock coatings would be a welcome development.

A hierarchical landscape geochemistry approach orders a way of understanding the geography of rock coatings. For example, first and foremost, bare rock faces must exist—exposed by geomorphic processes such as landsliding or glaciation. It is an obvious statement that without the exposure of bare rocks, we would not see subaerial exposures of rock coatings. Exposures of bare rock are most common in deserts and alpine settings because eroson of soils and regolith is generally faster than their production; thus, rock coatings are more commonly seen in these environments.

Second order controls exhibit where erosion exposes rock surfaces that had already developed rock coatings in the subsurface. The subaerial exposure of coatings that formed in rock fractures and soil cobbles is a second-order control, because a great many now-exposed coatings originated at depth within the rock.

Third order controls come into play when lithobionts colonize rock faces, and their rate of growth is often much faster than the inorganic rock coatings. Thus, lichens, fungi, and algae effectively outcompete slower growing inorganic rock coatings. Lithobionts are a third-order control, because they can dramatically alter the biogeochemistry of rock surfaces. This chemical change often dissolves inorganic coatings or can prevent them from accreting.

Fourth and fifth orders become relevant only if bare rock faces occur (1st order), if rock coatings are not exposed by an erosional event (2nd order), and if fast growing lithobionts do not grow over the rock face (3rd order). All three of these conditions must be met for the development of many of the subaerial rock coatings listed in Table 1. For example, the silica glaze on Stone Mountain (Fig. 1) could accrete, because a bare rock surface was not already coated by lithobions or an accretion formed originally in the subsurface.

The fourth and fifth orders of control focus on element abundance, element migration, geochemical flows, geochemical gradients, and geochemical barriers associated with different types of inorganic rock coatings. The fourth order focuses on the issue of whether or not the elemental ingredients of a rock coating are present and have a transport pathway to a site; for example, the iron and manganese present in rock varnish at Petra was mobilized down into sandstone pores (upper row in Fig. 1). However, just because the elements of rock coatings occur and are transported to a site does not mean that these elements will accrete.
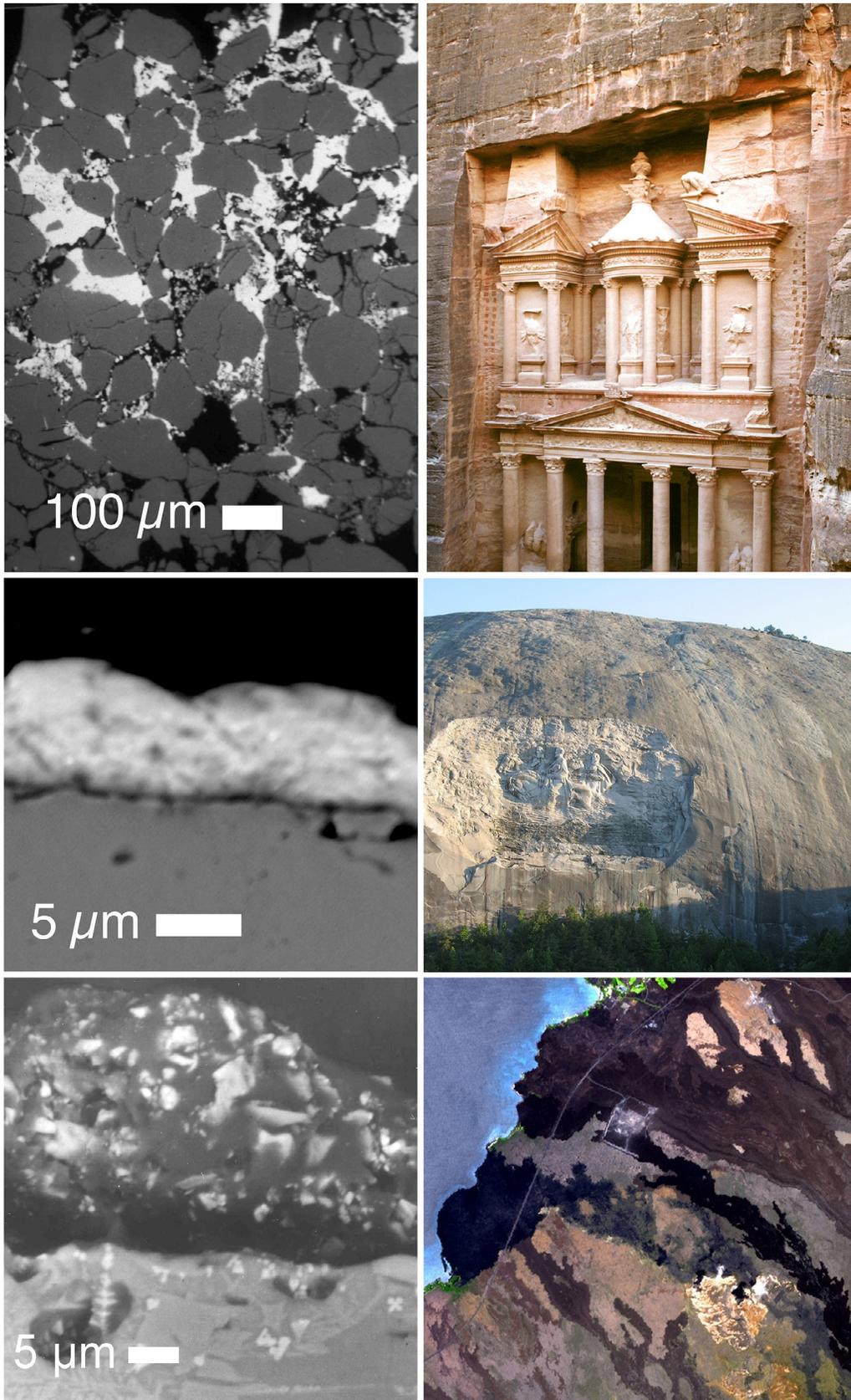
Fig. 1   Rock coatings alter the appearance of bare-rock landforms. The left column is the rock coating as seen through back-scattered electron (BSE) microscopy. The right column illustrates how thin rock coatings alters the visual appearance of rock. Top row: case hardening by heavy metals seen through darkens the appearance of a pink sandstone at Petra, Jordan. Middle row: calcium oxalate on quartz illustrates how even thin coatings create dark streaks on granodiorite at Stone Mountain, George, United States. Bottom row: silica glaze lightens the appearance of basalt flows as seen in an ASTER image of the rainshadow of Hualalai Volcano, Hawaii, courtesy of NASA (NASA, 2010), where even the 1859 Mauna Loa lava flow has a thin silica glaze coating. Scale in the right side images: top row height of Al-Kazneh is 40 m; middle row height of Stone Mountain is about 300 m; lower rock width of image is approximately 6 km.

The fifth order of control involves barriers to transport that fix the coating's constituents. The transport barrier might be physical, such as electrostatic or physical forces that hold dust particles together (Jordan, 1954; Bishop et al., 2002; Ganor et al., 2009). Another barrier could be geochemical, such as a change in pH/Eh oxidizing and fixing (NIAIST, 2005) iron in films. Still another barrier could be biological, exemplified by budding bacteria oxidizing manganese in rock varnish (Krinsley et al., 2017). Barriers to transport resulting in rock coatings can require a combination of biological, chemical, and physical processes.

2.1   1st Order control: Geomorphic stability

The first control on whether rock coatings occur is whether bare rock surfaces exist. Rock control is an important concept in geomorphology (Howard, 1994; Suzuki, 2002), and it is especially critical for rock coatings. After all, a cover of soil, vegetation, or regolith means that rock coatings have no subaerial exposure. Glaciers, waves, landslides, and overland flow in weathering-limited landscapes all exemplify geomorphic processes that can expose rocks to the atmosphere—the primary precondition for the occurrence of subaerial rock coatings.

Thus, the first order of control rests with geomorphic processes that generate bare rock surfaces for subaerial rock coatings (Fig. 2). A wide variety of geomorphic processes expose bedrock surfaces (Ehlen and Wohl, 2002; Molnar et al., 2007; Dorn, 2018; Israeli et al., 2021). Mass wasting, glacial, periglacial, volcanic, faulting, flooding, and coastal processes can all bring rocks into the subaerial environment. Bare exposures are most common in arid regions, because deserts are weathering-limited landscapes that have a paucity of vegetation (Gilbert, 1877).

2.2   2nd Order control: Subaerial exposure of subsurface coatings

Rock coatings often develop in the subsurface and are exposed at the surface by erosion of the overlying soil or rock material. For example, iron films develop on clasts in the B-horizon of soils (Haberland, 1975; Hayden, 1976; Pope and Miranda, 2016) and are then seen at the surface by soil erosion (Hunt and Wu, 2004). Similarly, iron films are found in fractures in weathering rinds in Burkina Faso that are later seen at the surface upon surface flaking (Metelka et al., 2015). Manganiferous rock varnish form in mountain soils (Ha-mung, 1968) and caves (Hill, 1982; Spilde et al., 2002; Northrup et al., 2003; Boston et al., 2008; White et al., 2009; Rossi et al., 2010; Gazquez et al., 2011; Gázquez et al., 2012; Lozano and Rossi, 2012). Weathered rock fractures are lined with Mn-Fe-rich rock varnish coatings (Weaver, 1978; Dorn and Oberlander, 1982; Douglas, 1987; Dorn and Meek, 1995; Kim et al., 2006; Krinsley et al., 2012; Li et al., 2017; Yu et al., 2017), dendrites or branching structures (Xu et al., 2010), and silica glazes (Milnes et al., 1991; Frazier and Graham, 2000). Clay-coated surfaces can be a common component of fractured bedrock (Frazier and Graham, 2000) and weathered minerals in general (Meunier et al., 2007). Fissures in less weathered bedrock host iron films, rock varnish, laminar calcrete, silica glaze, and heavy metals (Douglas, 1987; Dorn and Dragovich, 1990; Robinson and Williams, 1992; Mottershead and Pye, 1994; Villa et al., 1995). These coatings formed because transport pathways brought the necessary constituents, and because barriers to further transport fixed these constituents on fracture sides, in regolith, or on rock fragments in soils.

The landscape geochemistry setting of a rock coating can also change when human activity exposes a former subsurface coating (Cerveny et al., 2006), when a gully exposes regolith coatings (Goosens et al., 2015), or when scouring brings a soil clast to the surface (Palmer, 2002). Subsurface coatings brought into the subaerial environment through rock or soil erosion are extremely common, and my critique of many rock coatings articles is that they do not even consider a subsurface origin for the coating under study. The unstated assumption of much research is that just because a coating is currently found exposed to the atmosphere, it necessarily originated in that location.
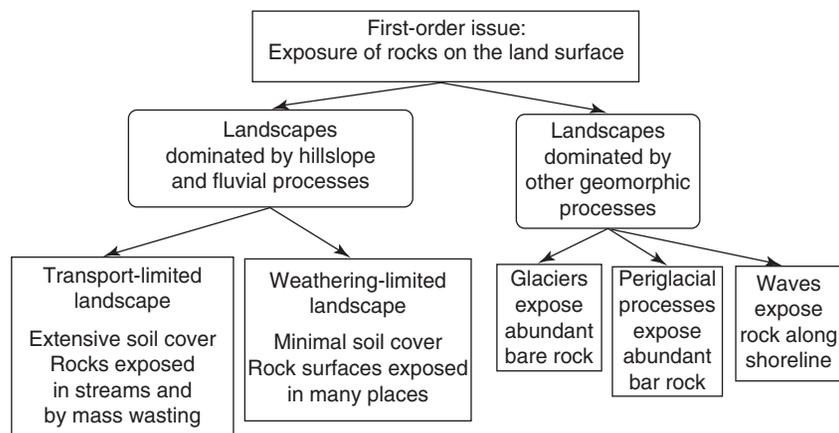

Fig. 2   Subaerial rock coatings only occur where bare rock faces have been exposed by geomorphic processes.
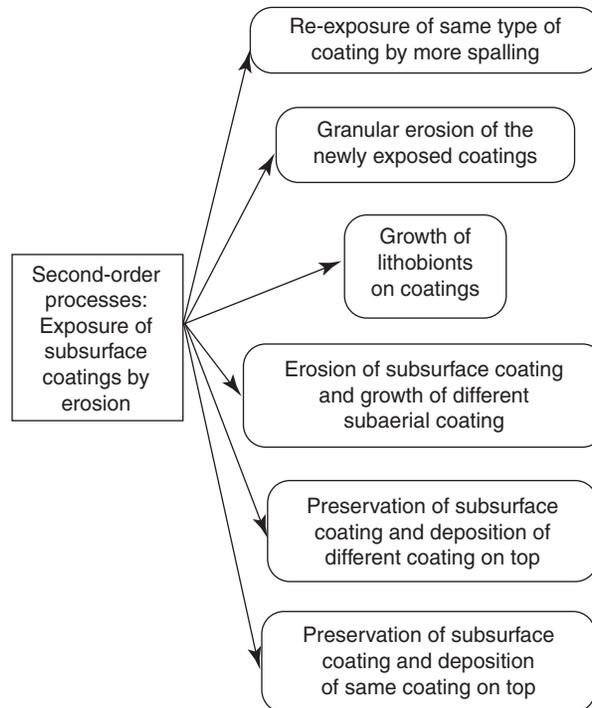
Fig. 3 Possible pathways of subsurface-formed coatings upon exposure in the subaerial environment. Further erosion may lead to exposure of other subsurface rock coatings. The joint face might erode by millimeter-scale flaking, removing the surficial coating. Lichens and other lithobionts might form on top of inorganic rock coatings, potentially leading to dissolution from the secretion of organic acids. A former subsurface coating might be dissolved by carbonic acid in rainwater, freeing up the surface for the growth of a subaerial coating more in equilibrium with the surficial environment. A new rock coating might form, or, in some cases, the same rock coating will continue to accrete.
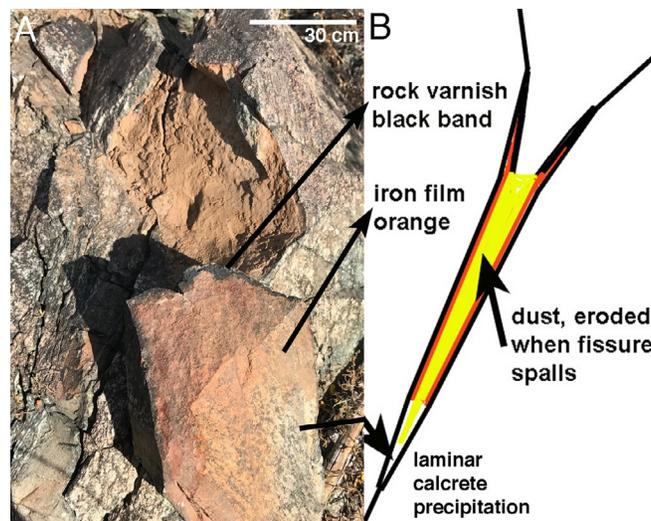

Fig. 4 Rock coating sequence found on the walls of desert rock fractures. (A) This fissure was pried open, exposing dust and weathered rock fragments. Carbonate leached from desert dust reprecipitates as laminar calcrete skins deeper in the rock fracture. An orange, iron-rich coating forms where dust is in constant contact with fissure sides. (B) Centimeter-scale band of black rock varnish rims the outer edge of the fracture where the dust has been washed away by infiltrating overland flow.

Upon exposure in the subaerial environment, what were once subsurface coatings can experience several possible futures, diagrammed in Fig. 3. Consider, for example, rock coatings that are ubiquitous in fractures found in warm deserts (Fig. 4). A laminar calcrete skin precipitates where the fissures are the most narrow; as the fissures open up, orange iron films accrete; a centimeter-wide band of black rock varnish grows where the fissures are close enough to the surface for precipitation to seep in and wash dust from fissure sides (Dorn, 2011).
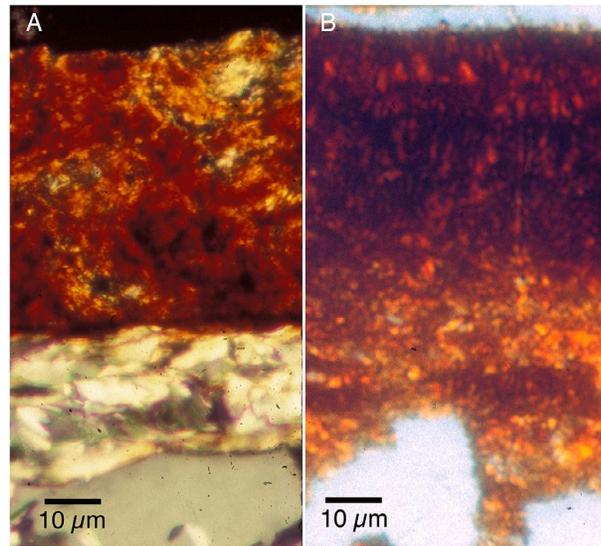
Fig. 5 Optical thin sections show how changes in landscape geochemistry alters rock coatings originally formed in desert fissures (cf. Fig. 4). (A) White calcrete first formed a coat over the gray quartz. Then, when the fissure opened wide enough to accumulate dust and weathered fragments, this dust fostered the formation of the orange film on top of the calcrete. (B) First, an iron film formed in the crevice. Then, the rock fracture opened wide enough to wash the accumulated dust away from the rock surface. This allowed the formation of a black rock varnish.

This colourful sequence of rock coatings found on the sides of rock fissures in warm and dusty deserts (Fig. 4) is modified as the landscape geochemical environment changes. As the fissure gradually opens wider, dust is washed from the walls of the fissure by precipitation, and this change allows the formation of manganese-rich rock varnish (Fig. 5B). With spalling, carbonic acid dissolves the laminar calcrete skins that are exposed, except where the iron film has already formed a protective covering (Fig. 5A). Spalling also promotes the formation of black manganese rock varnish over the orange surface, because the removal of the alkaline dust no longer inhibits microbial enhancement of manganese.

Joints or fractures in rocks in semi-arid environments often accumulate silica glaze that helps start the process of case hardening joint faces (Dorn, 1998). With erosion exposing joint faces to the subaerial environment, changes typically ensue. Fig. 6 documents two types of post-exposure changes seen in the semi-arid western USA. Both changes involve the accumulation rock varnish, followed by leaching of manganese and iron dissolved from the varnish—that then infiltrates into the underlying pores. Sometimes, the iron (with some manganese) infills pore spaces (Fig. 6A). In other cases, the manganese and iron combine with the silica glaze in the pores spaces and further contribute to case hardening the rock surface (Fig. 6B).
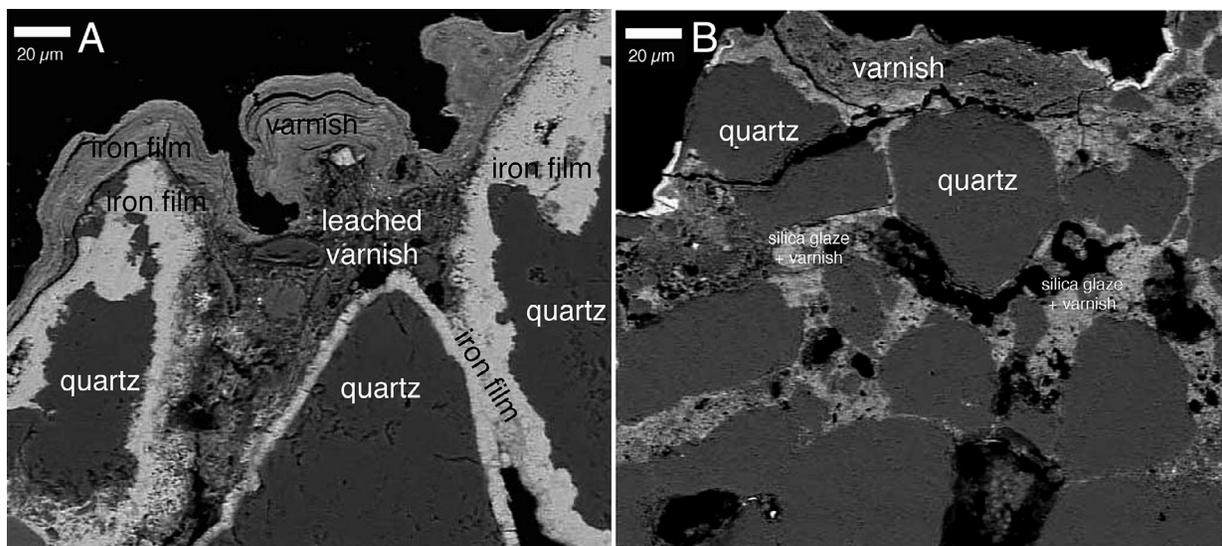

Fig. 6 Spalling of sandstone in Whoopup Canyon in Wyoming exposes silica glaze coat fractures. The change from subsurface fracture to subaerial surface enables rock varnish to accrete on top of the silica glaze. Image (A): BSE image shows case hardening by Fe (and some Mn) leached from the varnish. Image (B): BSE image presents Mn and Fe combining with silica glaze in pore spaces, forming a different type of case hardening.
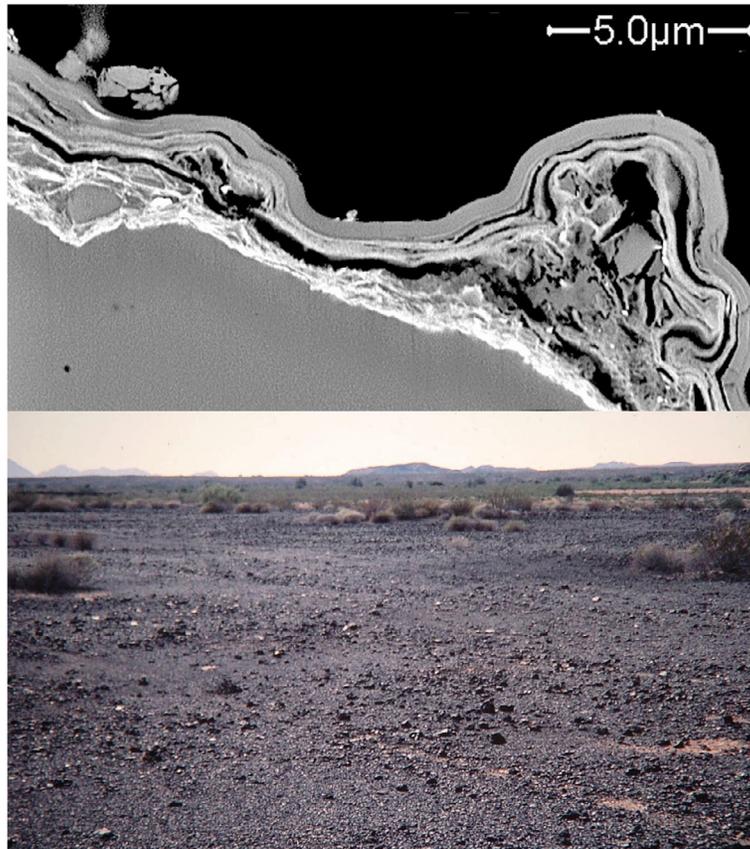
Fig. 7 Cobbles in desert pavements can develop a very shiny appearance. Some of this sheen, seen in the lower image from the Sierra Pinacate, Mexico, comes from silica glaze. In the upper BSE image, an iron film (brighter material) first formed on top of quartz on the side walls of a fissure. Then, dust accumulated in the fissure (fragments of gray material), and the dust was trapped by formation of more iron film. Then, the rock spalled and this former fissure was embedded in a desert pavement. A micron-thick layer of silica glaze then formed over the prior rock coatings at the ground-line band of the desert pavement cobble. This silica glaze allows some of the color of the underlying iron film to show through a very shiny appearance.

Another example of the influence of erosion altering the landscape geochemistry of subsurface-formed rock coatings comes from the spalling of a cobble in a Sonoran Desert pavement (Fig. 7). An iron film originally formed inside a rock fissure in a desert pavement cobble. Dust particles then adhered to the iron film, and iron film helped cement dust to the fissure side walls. Then, the rock split open, changing the landscape geochemical setting from a fissure to exposure at the soil line in a desert pavement. Desert pavement cobbles often develop a very shiny line at the soil line called a ground-line band (Engel and Sharp, 1958; Dorn and Oberlander, 1982). Ground-line bands are shiny, in part, because they develop coatings of silica glaze. Fig. 7 exemplifies that even a micron-thick layer of silica glaze can impart this sheen.

Erosional processes in deserts, both anthropogenic and natural, can expose carbonate crusts that become temporary subaerial coatings (Fig. 8). Originally formed in the Bk horizon of soils, the carbonate is slowly dissolved through interaction with carbonic acid in precipitation. A landscape geochemistry interpretation is that the geochemical barrier present in the soil no longer exists in the subaerial environment. Such changes in the position of pedogenic carbonate crusts have been used to analyze prehistoric geoglyphs and other earthen features (Cerveny et al., 2006).

Desert cobbles and small boulders in undisturbed settings host black manganese-rich rock varnish in a subaerial position, with an orange iron film forming where the clast remains in contact with the underlying alkaline soil (Cerveny et al., 2006). Rock coatings can offer a visually distinctive clue that soil erosion has been active, because seeing an abundance of orange iron films mean that clasts with the black rock varnish have been eroded. A study of variability in rock coatings along a single hillslope (Palmer, 2002) found greater amounts of soil erosion in the steepest portion and at the bottom of the disturbed hillslope in the Mojave Desert, resulting in the exposure of orange iron films at the surface (Fig. 9). Eventually, if erosion ceases or slows tremendously, black rock varnish will reform. However, Fig. 9 illustrates that the second order of control, erosion, plays a key role in determining the type of rock coating that is seen in disturbed settings.

Fig. 8   Carbonate crusts form on the underside of large boulders in Bk horizon in desert and semi-arid soils. Construction of a prehistoric rock cairn in the Panamint Valley, California, United States (upper image) and a 2010 debris flow (lower image) in metropolitan Phoenix, Arizona, United States expose pedogenically-formed carbonate crusts (arrows).
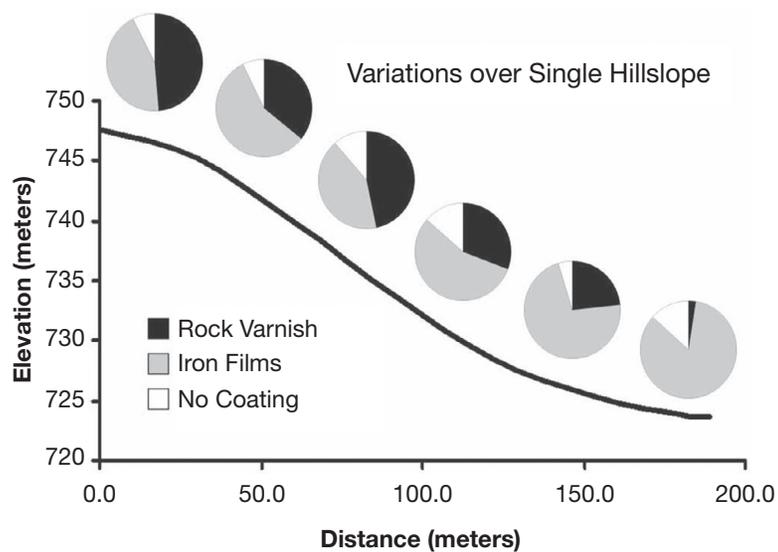

Fig. 9   A rock coating *catena* (Palmer, 2002) exemplifying how three different types of rock coatings change down a basalt hillslope in the Mojave Desert. The hillcrest has less soil erosion, and hence rock varnish dominates. More and more iron films occur further down the slope, reflecting greater soil erosion exposing the iron films that originally formed in the subsurface.

2.3   3rd Order control: Competition from lithobionts

Lithobiont coatings are organisms that live on the surface (epiliths), bore tubes into rocks (euendoliths), occupy fissures in rocks (chasmoendoliths), or live within the pore spaces of weathering rinds (cryptoendoliths) (Golubic et al., 1981). Lithobiont coatings thinner than a millimeter are classified as biofilms; those between 1 mm and 5 mm are biorinds; and coatings greater than 5 mm are called biocrusts (Viles, 1995; Gorbushina, 2007).

Lichens, fungi, and algae lithobiontic coatings grow much faster than most inorganic rock coatings such as rock varnish, iron films or silica glaze (Friedmann and Galun, 1974; Rundel, 1978; Golubic et al., 1981; Dragovich, 1987; Viles, 1995; Souza-Egipsy et al., 2004; Bhatnagar and Bhatnagar, 2005; Loso and Doak, 2006; Gadd, 2007, 2017; McMaster, 2012; Lacap-Bugler et al., 2017; Lavoie et al., 2017; Brewer and Fierer, 2018; Mergelov et al., 2018; Meslier et al., 2018; Mustoe, 2018; Powers et al., 2018; Genderjahn et al., 2021; Wieler et al., 2021). As a result, these subaerial organisms often dominate rock faces (Fig. 10). The third order of control, thus, involves conditions that control the growth of fast-growing lithobionts, where biofilm communities can grow in years to hundreds of years (Viles, 2001; Powers et al., 2018; Nir et al., 2019; Wieler et al., 2021).

One way that lithobionts take possession of a rock surface is through enhancing the weathering and erosion of rock material (Paradise, 1997; Lee and Parsons, 1999). Lichens grow on the surface, but also in pore spaces between mineral grains (Fig. 11). Increased spacing between mineral grains destabilizes the rock surface and spalling takes place. Part of the process involves enhanced dissolution of minerals under lichens (Aghamiri and Schwartzman, 2002; Gordon and Dorn, 2005a). Lichens are then able to recolonize these spalled surfaces much faster than inorganic coatings such as rock varnish or iron films. Another way that lithobionts replace other rock coatings is by biochemically dissolving (Dragovich, 1987) the pre-existing coating (Fig. 12).
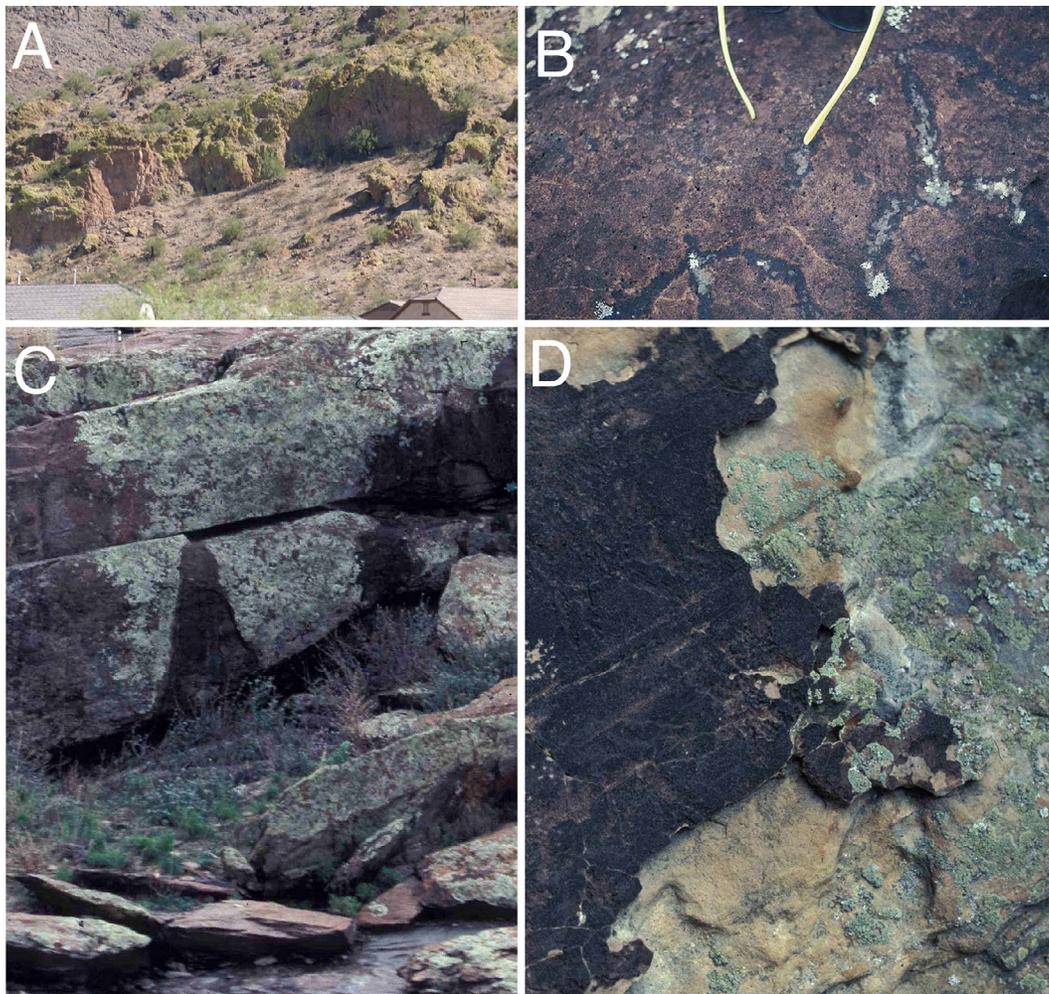

Fig. 10   Examples of lithobionts in different stages of covering subaerial rock surfaces. (A) Hillslope of welded tuff in central Arizona, United States where light green lichens cover rock surfaces that have remained stable for a few hundred years; image width ~100 m. (B) Dark-colored fungi colonize the surface of a former joint face, while lichens grow inside of engravings, Kaho'olawe Island, Hawaii, United States; sunglasses provide scale. (C) Lichens coating joint faces at a spring near Yunta, South Australia; image width ~3 m (D) Whoopup Canyon, Wyoming, United States, where lichens completely coat surfaces where the dark-colored heavy-metal case-hardened joint face has spalled away; image width ~20 cm.
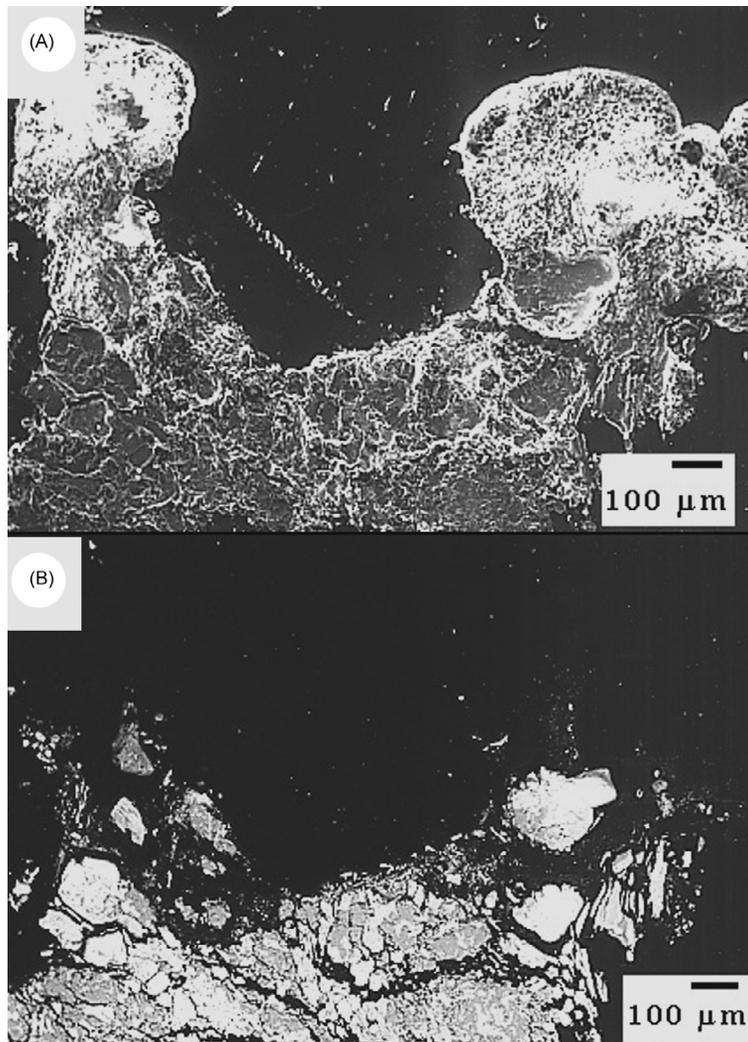
Fig. 11   Granodiorite inselberg surfaces at Garden Butte, Papago Park, central Arizona, United States, are dominated by lichens rather than rock varnish. Images A and B compare secondary electrons (A) to back-scattered (BSE) electrons (B). Note how the lichens seen with secondary electrons (A) penetrate into the rock along mineral boundaries and appear to enhance space between minerals, either mechanically or through chemical weathering.

Fig. 12   Lithobionts often secrete acids dissolve inorganic rock coatings. The left image shows basalt talus in the Mojave Desert, California, United States with inset photo of a petroglyph that was sampled for electron microscopy. The right image is a secondary electron microscope image from this inset showing a euendolith (tube boring) microcolonial fungi that is dissolving rock varnish.
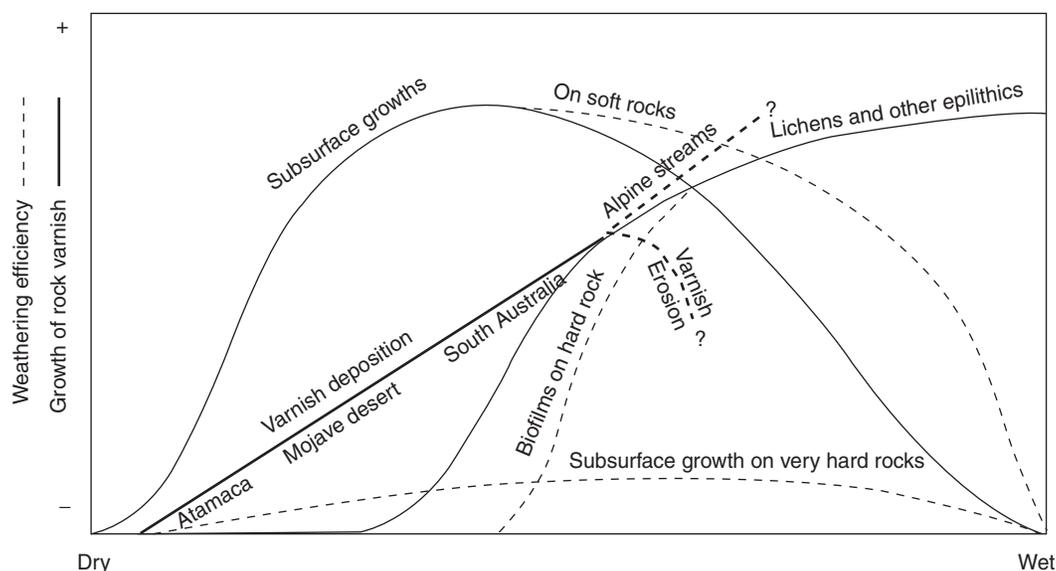
Fig. 13 A landscape geochemical conceptualization of how lithobionts and rock varnish interact together, adapted from Viles (1995) and Dorn and Oberlander (1982). Moisture plays a vital role in the growth of rock varnish and in the weathering efficiency of lithobionts. Secondary factors presented in this model are competition from lithobionts for rock varnish and rock hardness for lithobionts.

An example of the third order of control on rock coatings compares the behavior of lithobionts and another rock coating to the external forcing of moisture. Viles (1995, pp. 32) diagrammed lithobiont weathering as a function of moisture and hardness of the host rock. Dorn and Oberlander (1982) argued that the growth of rock varnish is influenced by moisture and competition from lithobionts. These two conceptualizations are combined in Fig. 13, linked through a common focus on moisture. Lichens are most common in moist settings, whereas much drier environments foster endoliths. Rock varnish survives best and grows the slowest in drier environments, but as moisture increases lithobionts biochemically dissolve more rapidly-forming varnish (e.g., Fig. 12).

Moisture conditions as diagrammed in Fig. 13, however, are not static. A site moves to the right and left on the diagram with microclimatic oscillations. A slight shift to wetter conditions can foster the colonization of lithobionts and result in varnish erosion. Considered from the perspective of Fig. 13, a site near the peak of varnish growth can shift into varnish erosion where acid-producing fungi have colonized rock varnish. The effect of such a change is seen in Fig. 14. While lithobionts chemically dissolve and erode pre-existing rock coatings and prevent the formation of many inorganic accretions, it is important to note that lithobionts can also stabilize rock surfaces by holding weathered fragments in place (Gehrmann et al., 1988; Kurtz and Netoff, 2001; Viles and Goudie, 2004). Lithobionts can also generate protective coatings of silica glaze (Lee and Parsons, 1999) and oxalate crusts (Souza-Egipsy et al., 2004).

2.4   4th Order control: Transport pathways

Rock coatings require a sufficient abundance of constituent elements and those elements are transported to accretion sites. Sometimes, the constituents are fairly ubiquitous—such as silica, clay minerals, and iron. For other rock coatings, the concentrations transported to a coating site are quite low and enhancement is required—such as with the manganese in rock varnish or iron in heavy metal skins (Huelin et al., 2006; Gazquez et al., 2012; Marnocha and Dixon, 2013; Municchia et al., 2016; Macholdt et al., 2017; Sharps et al., 2020). In other cases, while the overall abundance of material such as oxalate minerals might be low on a rock face, locally strong geochemical gradients might exist near a source of calcium oxalate (Steelman et al., 2021) such as lichens (Wadsten and Moberg, 1985). The 4th general control on the occurrence of rock coatings is, thus, the requirement that the constituents of a coating have a pathway of transport to a rock-surface site.

Some transport pathways are obvious. Nuclear fallout accumulating on mineral surfaces at Hiroshima Bay, Japan, have an obvious source and atmospheric pathway (Wannier et al., 2019). Pigments are applied to rock surfaces (Li et al., 2001; Hortola, 2005; Simionescu et al., 2009; Gallinaro and Zerboni, 2021) through anthropogenic transport (e.g., Figs. 15 and 16). Streaks of oxalate crust flowing down from oxalate-producing lichens at Stone Mountain (e.g., Fig. 1) reveal a visual trace of a transport pathway. A white streak formed over a Utah petroglyph panel corresponds with a thin coating of silica glaze (Fig. 17). Transport pathways can be dozens of kilometers for the dust that composes dust films and rock varnish, or very short in the case of iron and manganese mobilized from rock vanish and transported into pores to case harden the underlying rock (Figs. 6 and 14).

Transport of raw mineral ingredients involves two general preconditions. First, constituents must be present. Second, constituents must migrate to the rock face. For example, volcanic ash particles deliver the silica that then mixes with acidic volcanic rain and volcanic smog (vog) produces silica glazes within 250 years on Asama volcano, Japan (Nakatani et al., 2021). Bird droppings
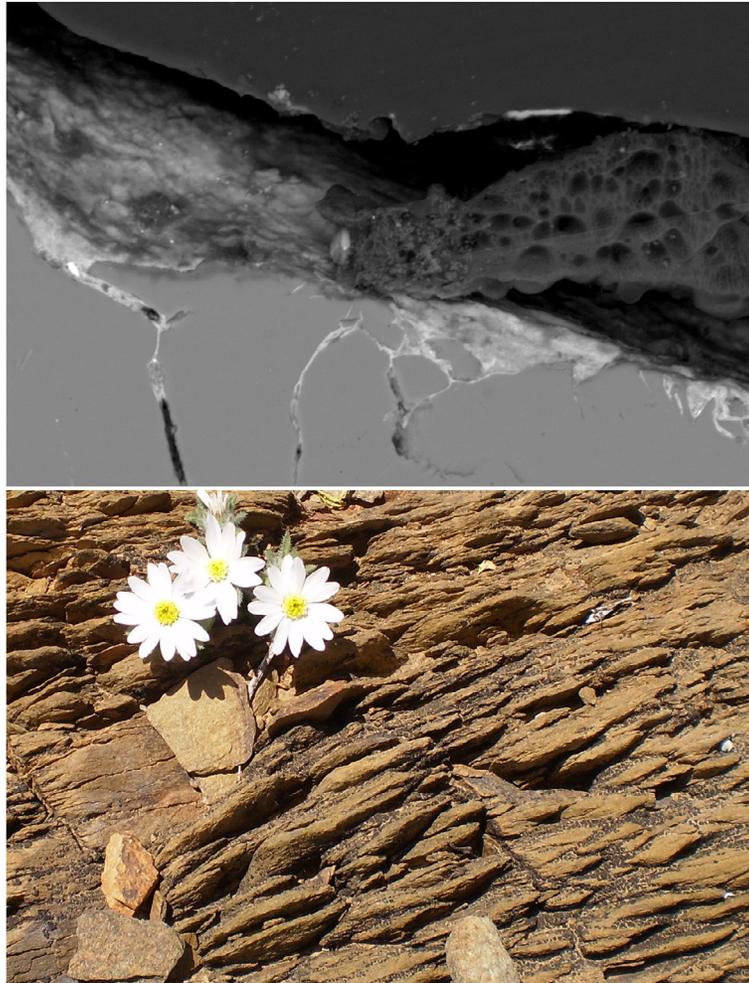
Fig. 14   Varnish and biofilms of fungi and lichens grow on schist (lower image, where flower width is 2 cm). At the present time, biofilms appear to be dissolving varnish, as illustrated in the BSE image (image width is $\sim$100 μm; the epoxy has separated from the fungi and dissolved varnish). The dissolving varnish then reprecipitates inside fractures, promoting case hardening with iron and manganese heavy metals. This example corresponds with the location of "varnish erosion" in Fig. 13, where biofilms are growing on hard rocks.

Fig. 15   Anthropogenic paint balls transported and applied to rock surfaces at South Mountain Park, Arizona, United States.
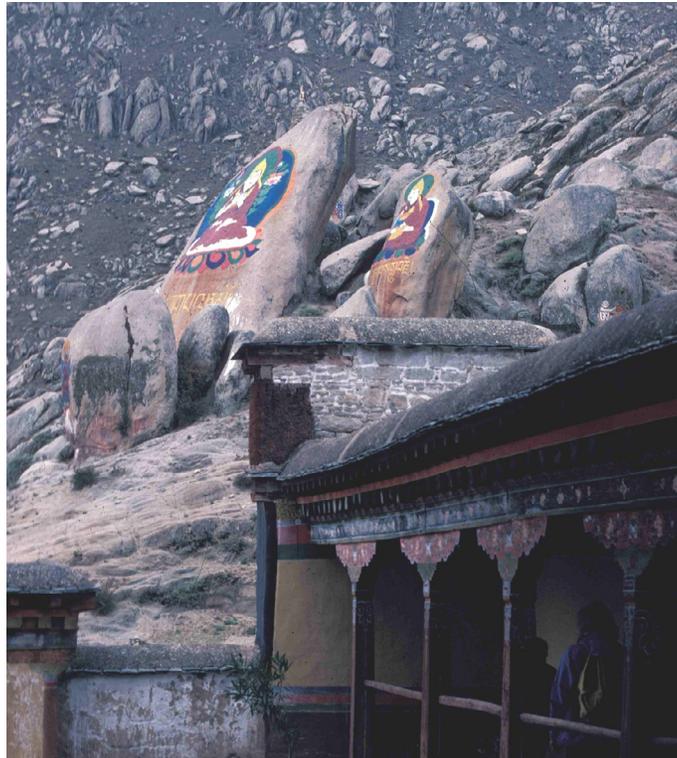
Fig. 16   Anthropogenic pigments applied next to the DeBrung Monastery, Tibet.
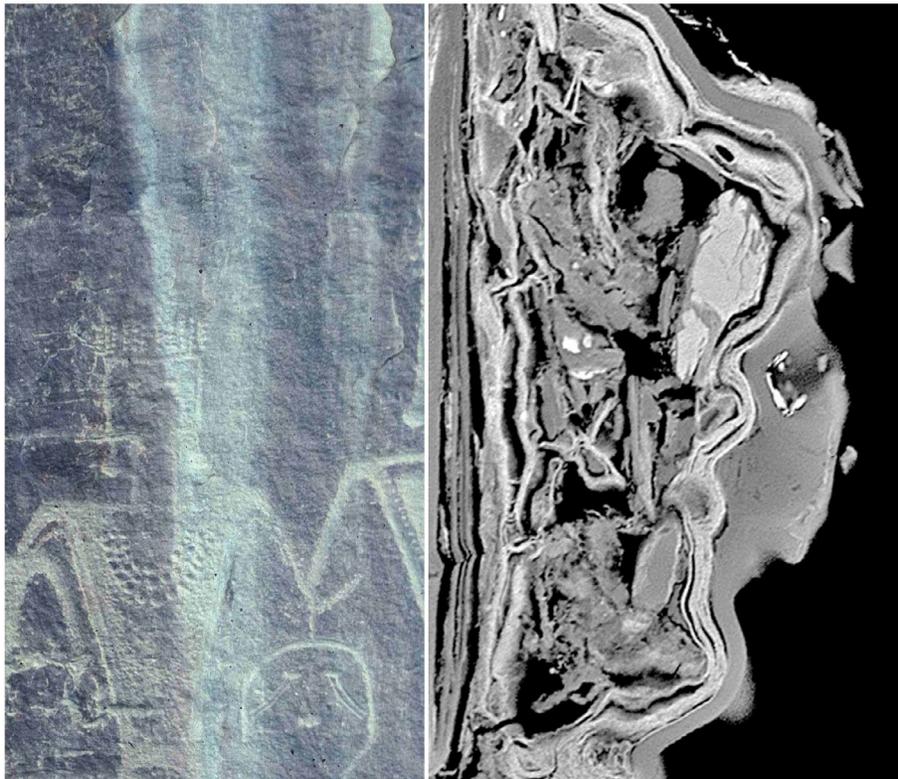
Fig. 17   Streak of silica glaze formed over a petroglyph panel at McKonkey Ranch, Utah, United States. The white streak was sampled above the engraving on a natural joint face. The BSE image shows three types of rock coatings, where the host rock is on the left side of the electron micrograph. On top of gray quartz is a thin layer of rock varnish (bright material) formed. Then, on top of that varnish is dust film loosely cemented with iron and manganese. On top of this rests the water-streak silica glaze. The source of the water-mobilized and transported silica appears to be a rock spall that redirected overland flow. The photograph is about 2 m in length, and the BSE image width is 10 μm.
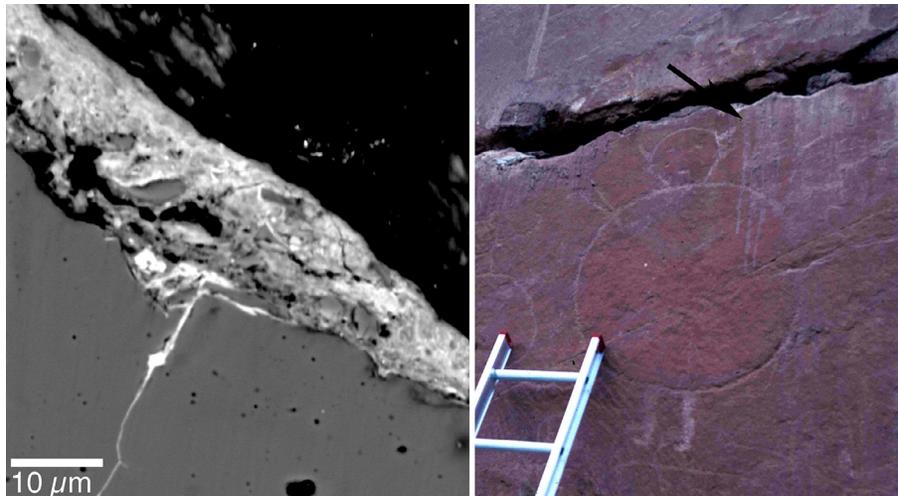
Fig. 18   A sandstone face at Medicine Lodge Creek, Wyoming, United States, has a fracture occupied by birds. Droppings are mobilized and drip down the rock art panel. The back-scatter electron microscope image shows phosphate mixing with detrital rock fragments, perhaps transported by water flow.

(Arocena and Hall, 2003; Gomez-Heras et al., 2004) or microorganisms (Konhauser et al., 1994) generate the requisite material for a phosphate skin. Then, phosphates are mobilized and reprecipitated (Fig. 18). In another example, the formation of silica glazes on granite building stones in Rio de Janeiro first requires dust deposition; then, silica is mobilized from the dust to reprecipitate as silica glaze (Smith et al., 2007). Deposited particulate matter, in general, appears to be a key agent in the formation of pollution-related coatings in urban settings where the general step is particulate deposition, followed by complex interactions that result in the net migration of elements from particulates into a rock coating (McAlister et al., 2006).

Salt crust formation exemplifies how multiple transport steps can involve very different processes (Oguchi et al., 2002). Salt crusts occur on a variety of weathered surfaces seen in satellite imagery (Berger et al., 2015), in rock shelters (Roberts et al., 2018), on churches near coastlines (Gaylarde et al., 2017), or natural rock surfaces near salt playas such as Mushroom Rock in Death Valley. In the case of Mushroom Rock in Death Valley (Meek and Dorn, 2000), the salt was first transported by wind from the salt playa to the soil adjacent to the talus boulder. Then, salt was dissolved in precipitation and moved by capillary action up the side of the boulder to precipitate as salt crusts (Fig. 19).

Multiple transport pathways are key to the formation of black crusts found on marble tombstones and limestone buildings in humid regions experiencing anthropogenic pollution. Sulfate and oxalate crusts both occur on such surfaces as Fig. 20. Sulfate crusts can occur naturally (Wen et al., 2020). Perhaps more commonly, sulfur from carbon fuel combustion interacts with the host carbonate to produce gypsum sulfate crusts (Potgieter-Vermaak et al., 2004). Then, this gypsum is transported microns to millimeters on the rock surface to contribute to the development of inorganic deposits that could be microbial produced (Gaylarde et al., 2017).

The deposition of sulfate crust occurs in tandem with dissolution of the limestone, but the style of the accretion can vary (Fig. 21). In some cases, a thicker crust of several hundred micrometers forms as the gypsum replaces the limestone (Vergès-Belmin et al., 1993) through a process by which sulfate-rich solutions migrate outward from the rock in the early stages of surface desiccation (Smith, 1994). In other cases, the sulfate crust manifests itself as a mix of gypsum needles and soot over karren (Camuffo et al., 1983).

Sometimes, the lack of a transport pathway for a key ingredient can determine what type of rock coating accretes. This is especially true for rock varnish. Black streaks across sandstone surfaces of the Colorado Plateau are almost always attributed by US National Park rangers to rock varnish, but this is often incorrect. These water-flow deposits often lack clay minerals. Since clays are vital to the formation of rock varnish (Potter and Rossman, 1977; Krinsley et al., 1995; Krinsley, 1998; Dorn, 2007), the manganese and iron deposited without the clays results in a heavy metal skin (Fig. 22). Another example comes from Hawaii. Silica glaze forms on the rainshadow side of the island of Hawaii (Fig. 1), in part because of the paucity of clay mineral transport to basalt flow surfaces.

2.5   5th Order control: Barriers to transport

Physical, chemical, and biological barriers all can halt the transport of elements, resulting in the accretion of rock coatings. This fifth order of control is not ranked higher, because the other controls can prevent the occurrence of a coating, even if a barrier to transport exists. For example, even though dust is ubiquitous in warm deserts (Goudie, 1978) and coatings occur where electrostatic or physical forces hold dust particles together (Jordan, 1954; Bishop et al., 2002; Ganor et al., 2009), the lack of bare rock surfaces (1st order), the exposure of a subsurface coating (2nd order), the growth of lithobionts (3rd order), or the transport of other materials by
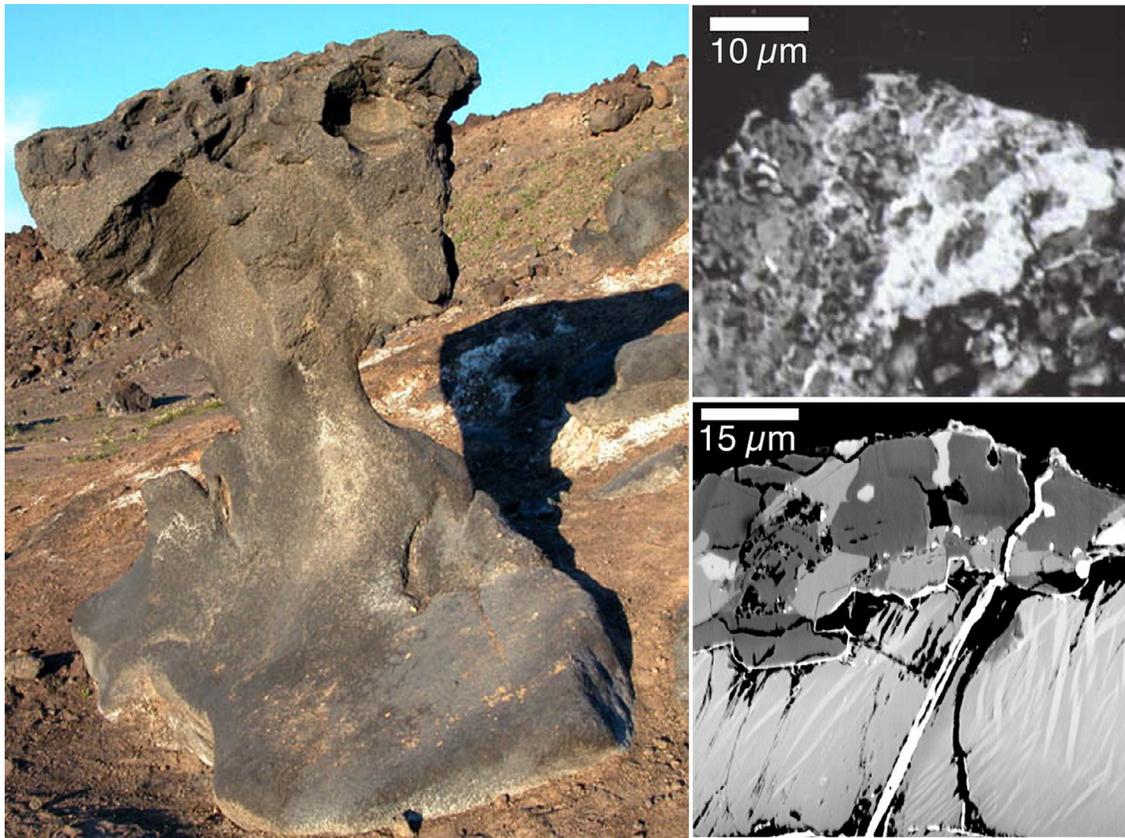
Fig. 19 Barium sulfate, sodium chloride, calcium sulfate, and strontium sulfate all weathers ∼3.5 m tall Mushroom Rock in Death Valley, California, United States. The BSE micrographs on the right show a barium sulfate crust as the brighter material both fragmenting the basalt and covering mineral surfaces. The bright white in these images are barite and minerals are weathered basalt minerals.

Fig. 20 Sulfate crust on marble tombstone in the Old Fellowship Cemetary (sic) in Atlanta, Georgia, United States.
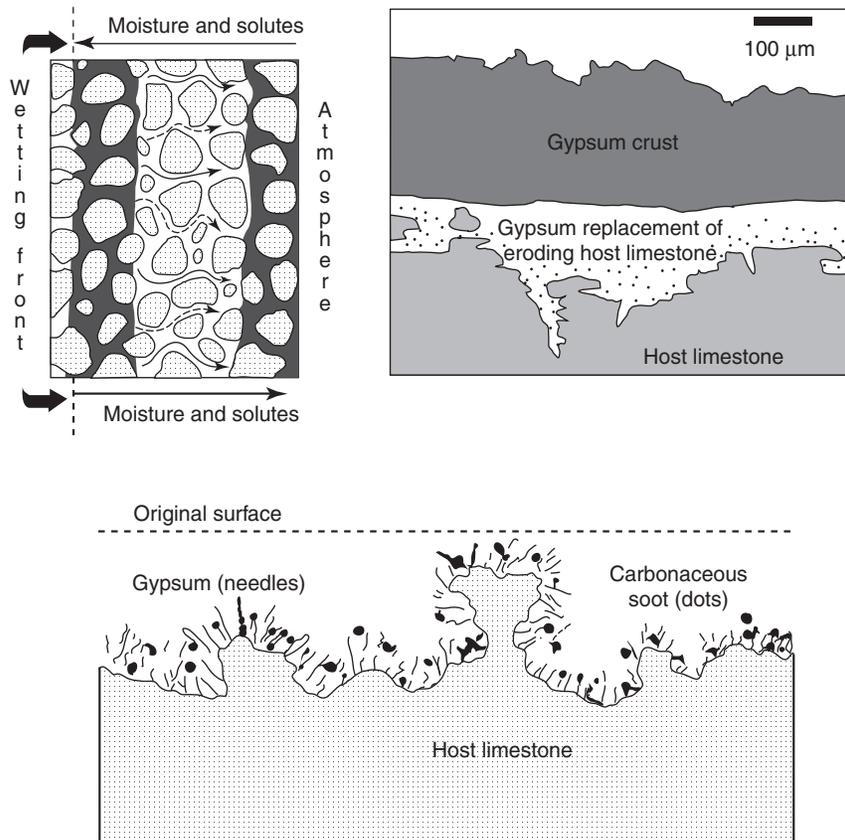
Fig. 21   Pollution-generated gypsum crusts can replace the host limestone through flow of sulfate-rich solutions migrating from the rock, and they can exist as needles over a dissolving surface.
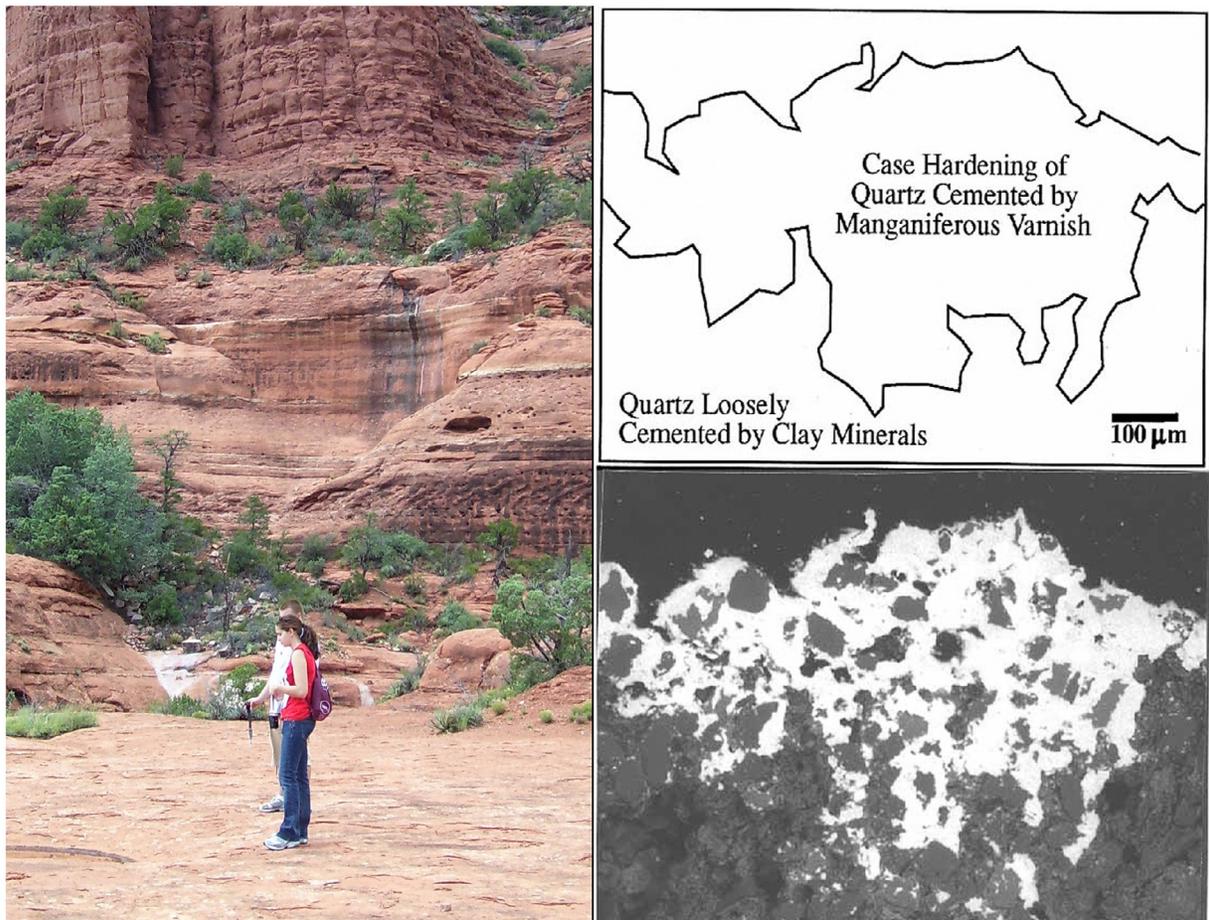
Fig. 22   Waterflow streaks can sometimes be fungi, lichens, heavy metal skins, and sometimes rock varnish. In this case, streaks are heavy metal skins that impregnate the sandstone of Sedona, at Schnebly Hill Road, Arizona, United States.
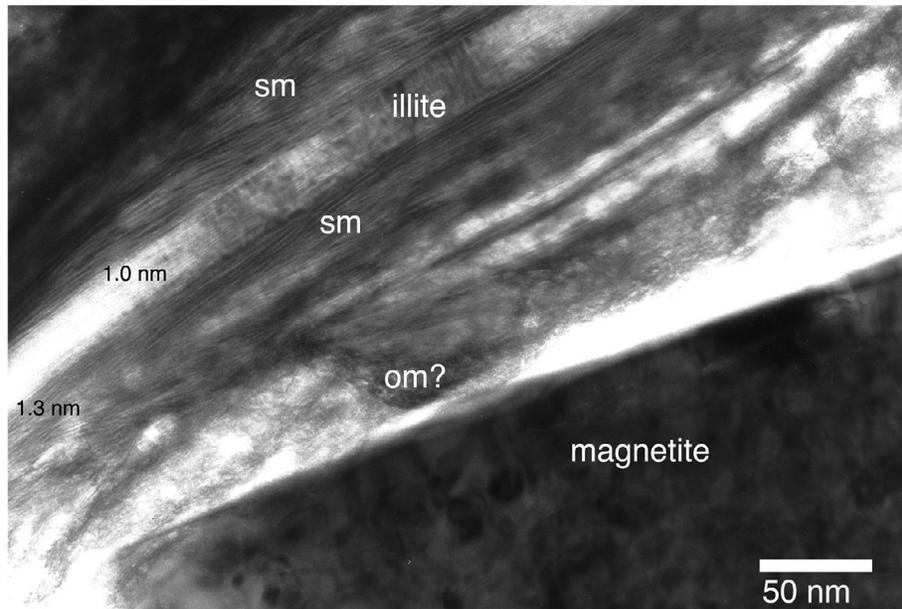
Fig. 23 High resolution transmission electron microscope image of a dust film that has been preserved inside a partially opened rock crevice. Its position protects the coating from being washed away by incident precipitation. The sample was collected from a granodiorite surface, South Mountain, central Arizona. The nature of the clays in this dust film show an orientation parallel to magnetite surface of the wall of the crevice. There is a mixture of illite and smectite (sm). The illite has a spacing of 1.0 nm. The darker portions of the smectite are too thick for spacing measurement, but the thinner portions show spacing of 1.3 nm. There may also be organic matter (OM?) as a part of the dust film.

water or wind (4th order) can all interfere with the occurrence of coating, for example a coating of dust on a rock surface (Fig. 23). This section presents examples from the coatings of dust films, silica glaze, rock varnish, and carbonate crusts.

Physical and chemical barriers often work in tandem to generate inorganic rock coatings, as it the case for silica glaze (Chemtob and Rossman, 2014; Aftabi and Atapour, 2018). Dorn (1998) proposed that silica glaze formation starts with soluble Al-Si complexes $[Al(OSi(OH)^3)^{2+}]$ that are common at the water-rock interface (Browne and Driscoll, 1992). Dew or frost deposition supplies sufficient moisture to mobilize Al-Si complexes, where the transition between complete and partial wetting on silica surfaces is about 20–70 nm (Zorin et al., 1992; Churaev, 2003). Crossing this physical transition would result in the deposition of silica with particles in the size range of 20–70 nm. High resolution transmission electron microscopy (HRTEM) finds evidence of spheroids in this size range in silica glaze (Fig. 24), an observation consistent with this model of silica glaze formation (Langworthy et al., 2010).

Another example of the 5th hierarchy of barrier to transport comes from rock varnish. Rock varnish formation begins with physical barriers of electrostatic or physical forces holding dust particles together on subaerial surfaces (Jordan, 1954; Bishop et al., 2002;
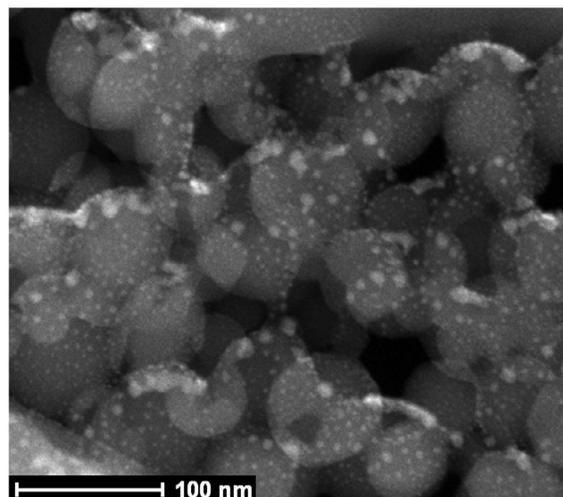

Fig. 24 HRTEM image of silica glaze spheroids in a sample from the Ashikule Basin, Tibetan Plateau. The bright dots are artifacts of sample preparation.
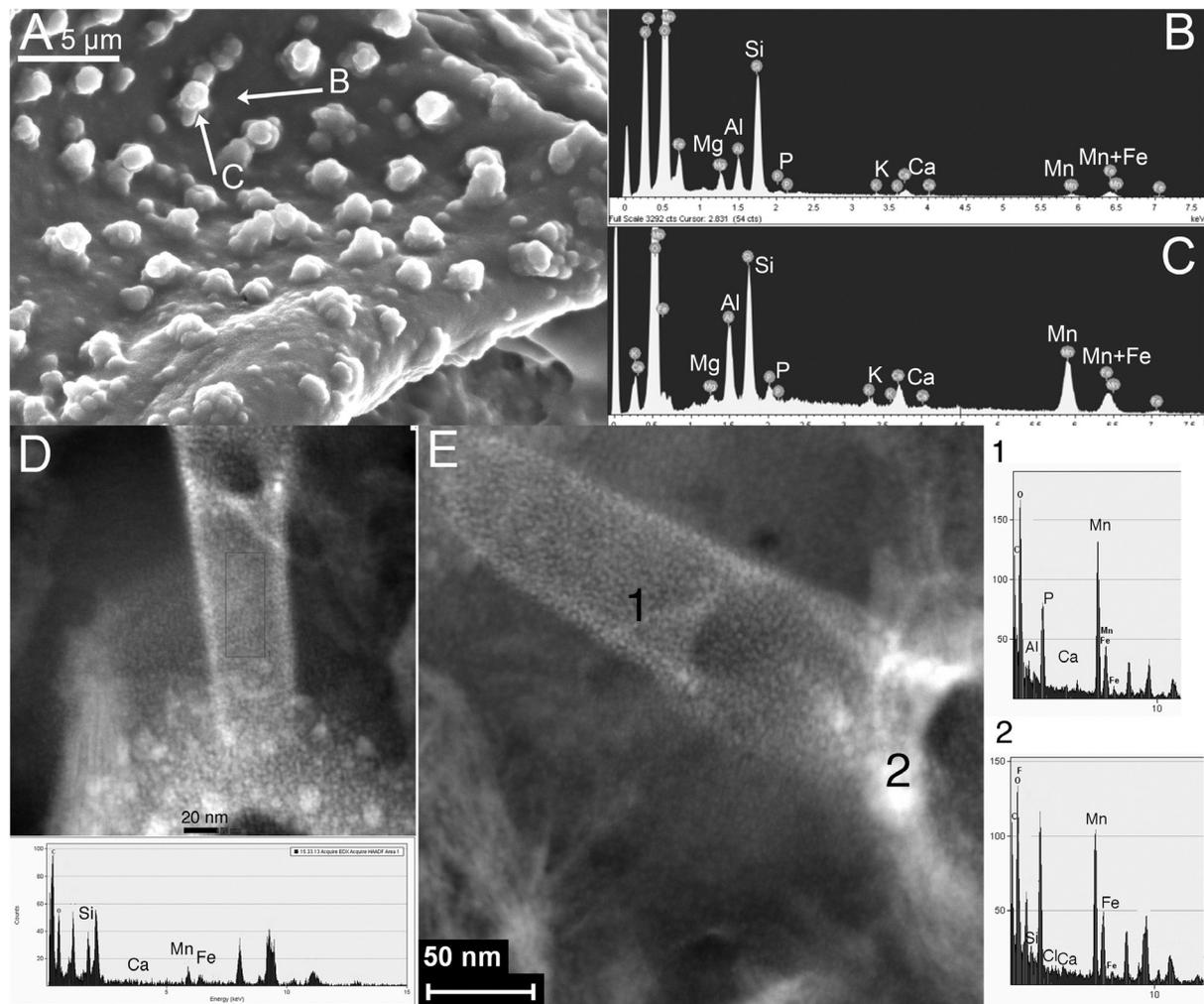
Fig. 25   The only directly observed process of varnish formation involves budding bacteria (Dorn and Oberlander, 1982; Dorn, 1998; Krinsley et al., 2017). All other proposed mechanisms of varnish formation are either deduced or are just theoretical. Image (A): Budding bacteria growing on Negev Desert varnish collected 2 weeks after a winter rain, where image (B) shows the energy dispersive spectra (EDS) of the surrounding varnish compared with image (C) showing much higher Mn-Fe concentrations on the sheath of the budding cell. Images (D) and (E) show high resolution perspective on fixation of Mn and Fe. (A) Electron microscope image of budding bacteria concentrating Mn and Fe (Krinsley et al., 2017), where a budding hyphae emerges from cocci bacterial forms. The EDS in D is on the emerging hyphae, while EDS 1 and 2 in image (E) were collected from the hyphae and cocci, respectively.

Ganor et al., 2009). Then, the biological action of bacteria concentrate manganese and iron (Dorn and Oberlander, 1981; Hungate et al., 1987; Dorn, 2007; Northup et al., 2010; Wang et al., 2011; Vázquez-Ortega and Fein, 2017). Some of the bacterial sheaths become microfossils (Dorn and Meek, 1995; Dorn, 1998; Krinsley, 1998; Krinsley et al., 2012, 2017) that then dissolve. Decay of the Mn-Fe casts mobilize nanometer fragments. Physiochemical fixation takes place only a few nanometers away when the oxides are fixed into mixed-layered clays (Potter, 1979). HRTEM imagery (e.g., Fig. 25) shows Mn and Fe inserted into mixed-layered clays. Potter (1979, pp. 174–175) hypothesized:

> "Deposition of the manganese and iron oxides within the clay matrix might then cement the clay layer…the hexagonal arrangement of the oxygens in either the tetrahedral or octahedral layers of the clay minerals could form a suitable template for crystallization of the layered structures of birnessite. The average 0–0 distance of the tetrahedral layer is 3.00 Å in illite-montmorillonite mixed-layered clays, which differs only 3.4 percent from the 2.90 Å distance of the hexagonally closed-packed oxygens in birnessite…"

Budding bacteria are the key agents that enhance both Mn and Fe (Dorn and Oberlander, 1982; Krinsley et al., 2017). Mn and Fe accumulate on the surfaces of cells and hyphae (Fig. 25). Then, ongoing diagenesis breaks apart these cell encrustations into nanoscale granules (Krinsley, 1998) that are then remobilized and reprecipitated among the mixed-layer clays in a process first explained by Potter (1979, 174–175):

> "Deposition of the manganese and iron oxides within the clay matrix might then cement the clay layer…the hexagonal arrangement of the oxygen in either the tetrahedral or octahedral layers of the clay minerals could form a suitable template for crystallization of the layered structures of birnessite."

McKeown and Post (2001, pp. 712) later elaborated that ongoing disequilibria exists even after the varnish formed:

> "[e]ven if analysis methods are improved, the situation will remain complicated by the flexibility and great variety of Mn oxide structures. The common elements of these structures enable them to easily intergrow with and transform with one another".

Thus, while budding bacteria originally enhance the Mn-Fe, it is the geochemical dissolution at the nanoscale and subsequent reprecipitation of oxyhydroxides in clays that results in varnish formation. It is important to stress, however, that shifts at the nanoscale do not create instability (Krinsley et al., 2013) in the laminations seen at the micron scale that are stable for tens of millennia (Liu et al., 2013; Liu and Broecker, 2013; Liu, 2021)—much like cars moving around inside a parking lot do not change the lot itself. The combination of budding bacteria concentrating Mn (and Fe) along with abiotic fixation is called the polygenetic model of varnish formation (Dorn, 1998). Almost all of the other explanations for varnish formation do not include a rate-limiting step and hence fall prey to this "varnish rate paradox."

Sunlight was once thought to be a key to varnish formation (Blake, 1905), and new research indicates that varnish has photoelectric properties (Lu et al., 2019; Xu et al., 2019). A new idea for varnish formation that does account for the slow rate of varnishing in hot deserts involves photo-catalysis (Otter et al., 2020). Sunlight is also a critical aspect of the hypothesis that cyanobacteria are the key to varnish formation, either via Mn-oxidation (Krumbein, 1969) or as a catalytic antioxidant (Lingappa et al., 2021). The difficulty with these ideas involving sunlight is that Mn-Fe rock varnish forms in settings that are not exposed to any sunlight. The same manganiferous rock varnish observed in warm deserts also develops on rock surfaces within unexposed mountain soils (Ha-mung, 1968). Rock fractures that are unopened are similarly lined with Mn-Fe-rich rock varnish (Weaver, 1978; Dorn and Oberlander, 1982; Douglas, 1987; Dorn and Meek, 1995; Kim et al., 2006; Krinsley et al., 2012; Li et al., 2017; Yu et al., 2017). Mn-Fe coatings also develop in cave settings not exposed to sunlight (Hill, 1982; White et al., 2009; Rossi et al., 2010; Gazquez et al., 2011; Gázquez et al., 2012; Lozano and Rossi, 2012) and are also considered to be rock varnish (Spilde et al., 2002; Northrup et al., 2003; Boston et al., 2008). Unfortunately, none of these new ideas of varnish formation involving sunlight considered this prior literature; if they had considered this flaw in their reasoning, the authors might have argued that the varnish they studied in subaerial environments and the varnish found in the subsurface could possibly form in different ways—a notion not well shaved by Occam's Razor.

Many other models of varnish formation have been proposed. Some favor Mn-enrichment through purely abiotic processes such as small Eh/pH fluctuations (Engel and Sharp, 1958; Soleilhavoup, 2011; Goldsmith et al., 2014). These abiotic processes would generate varnishes $100 \times$ to $10,000 \times$ faster than observed (Dorn and Krinsley, 2011; Krinsley et al., 2017).

Organisms other than budding bacteria have been invoked (Krumbein, 1969; Krumbein and Jens, 1981; Taylor-George et al., 1983; Palmer et al., 1985; Northup et al., 2010; Lingappa et al., 2021). Among the problems with these competing explanations are the lack of fossil remains of these organisms.

Still others point to phylogenetic insight about organisms growing on and in varnish (Eppard et al., 1996; Perry et al., 2004; Kuhlman et al., 2005, 2006a,b, 2008; Benzerara et al., 2006; Northup et al., 2010; Esposito et al., 2015, 2019; Lang-Yona et al., 2018; Martínez-Pabello et al., 2021). If even a fraction of the studied microbial community growing in and on varnish resulted in varnish formation, rates of accretion would be orders of magnitude higher than observed for the warm desert sites studied (Krinsley et al., 2017).

The polygenetic origin of varnish is the only hypothesis that has presented: (i) direct in situ evidence of the process of Mn-Fe enrichment (e.g., Fig. 25) in *both* surface settings exposed to light *and* subsurface settings; (ii) contains microfossils (and more importantly) pieces of microfossils that are being incorporated into varnish via diagenesis (Krinsley, 1998); (iii) explains observed varnish textures (Krinsley, 1998); and (iv) explains slow rates of varnish growth in warm deserts (and also some faster growth rates in non-desert environments) (Dorn and Krinsley, 2011; Krinsley et al., 2017). The only hypothesis that meets these criteria involves the rare event of the growth of budding bacteria (Fig. 25) where rare fossil evidence exists of the decaying remnants of budding sheaths have been directly observed (Dorn and Meek, 1995; Dorn, 1998; Krinsley, 1998; Krinsley et al., 2012, 2017).

Rock varnish formation, then, appears to be the result of a sequence of barriers and nanometer-scale transport: first, physical barriers to the migration of first dust that supplies clay minerals; second, biological barriers that enhance manganese and iron; third, Mn and Fe are transported nanometers to adjacent clay minerals; and fourth, the physiochemical processes cement clay minerals to the rock and to prior varnish. This is the polygenetic model of rock varnish formation (Dorn, 1998).

Another example of the 5th order of control of barrier to transport comes from carbonate crusts. Although carbonate crusts do not necessarily require such a complex sequence as rock varnish, they can form from physical, chemical, or biological barriers to transport of carbonate (Fig. 26). Carbonate rocks in the Negev Desert, for example, interact with microorganisms to produce laminated carbonate coatings (Wieler et al., 2019). Tufa and other types of carbonate crusts are known to form from both biotic and chemical processes that create barriers to further transport (Pentecost, 1985; Pedley, 1990; Viles and Goudie, 1990; Benson, 1994; Arp et al., 1999; Carter et al., 2003; Yoshikawa et al., 2006). These deposits have been used to place age constraints on rock art and hence can remain stable enough in some settings (Benson et al., 2013). Marine carbonate cementing rock surfaces in coastal areas appear to be related to activity of algae and cyanobacteria (Krumbein, 1979; Kendall et al., 1994). The physical barrier of evaporation can also form carbonate crusts (Schlesinger, 1985).
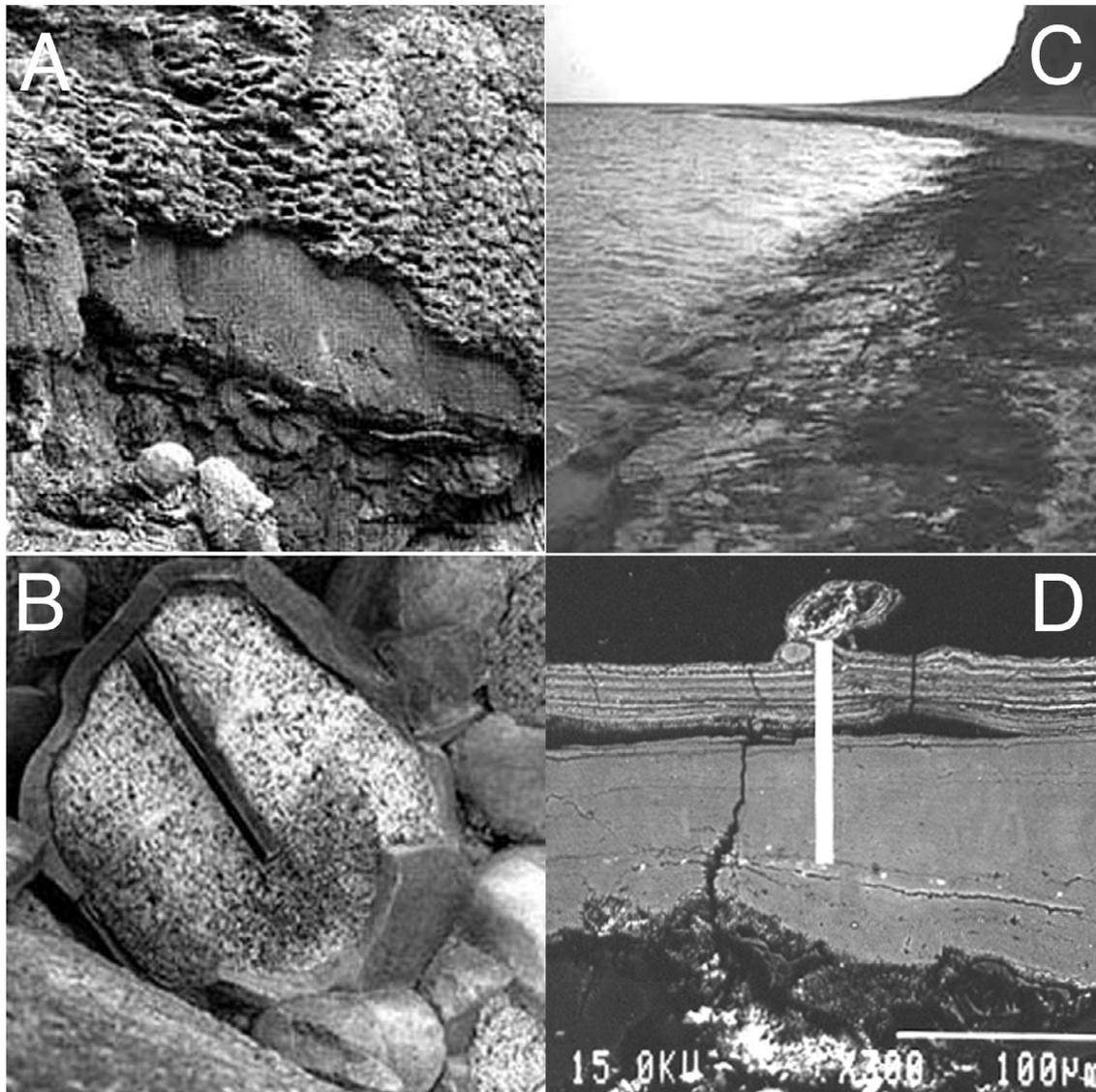
Fig. 26   Carbonate crusts formation in different environments. Images (A) and (B) show tufa formed in a lacustrine environment at Pyramid Lake, Nevada, United States, generating centimeter-scale crusts over rock surfaces. Image (C) illustrates a biogenic carbonate crust of beachrock ~2 m wide and tens of centimeters thick along the northeastern shore of the Sinai Peninsula, Egypt. (D) BSE image shows carbonate crust formed as a result of sprinkler water evaporating on a tombstone in Phoenix, Arizona, United States.

Barriers to elemental migration can shift, resulting in very different types of rock coatings, even over scales of tens of nanometers (Fig. 27). In a sample from the dusty and alkaline Ashikule Basin, Tibet, layered varnish rests on top of and underneath silica glaze composed of spheroids. In this high resolution transmission electron microscopy (HRTEM) image, varnish rests distinctly on the underlying rock and silica glaze spheroids makes a distinct contact with the varnish both underneath and above the silica. Energy-dispersive X-ray spectroscopy (EDS) analysis of the middle zone reveals that the spheroids are composed of Si and O, similar to Fig. 24. The shifting geochemical barrier could have been something as subtle deposition of alkaline dust changing the pH from near-neutral conditions favoring rock varnish formation to higher pH conditions favoring silica glaze formation, and then back again to near-neutral pH values.

Geochemical barriers can shift over short or long time scales, ranging from hours to thousands of years. Temporary rock coatings of ice can melt within a day (Hetu et al., 1994). Organic coatings on andesite volcanic blocks form during the final stages of the solidification of a lava flow, resulting in the coalification of plant material (Donoghue et al., 2009). Acid-fog generates coatings that mix silica glaze and jarosite, formed from evaporative processes (Shiffman et al., 2006). Iron films transform from ferrihydrite to goethite (Raiswell et al., 2009) under glaciers and ice sheets over periods of less than 100 years. Silica glazes can form within a few decades (Gordon and Dorn, 2005b) and can alter lava flow appearances dramatically within centuries to millennia (Fig. 1). Rock varnishes accrete evidence of millennial-scale climatic change through shifting geochemical barriers (Fig. 28); time periods with
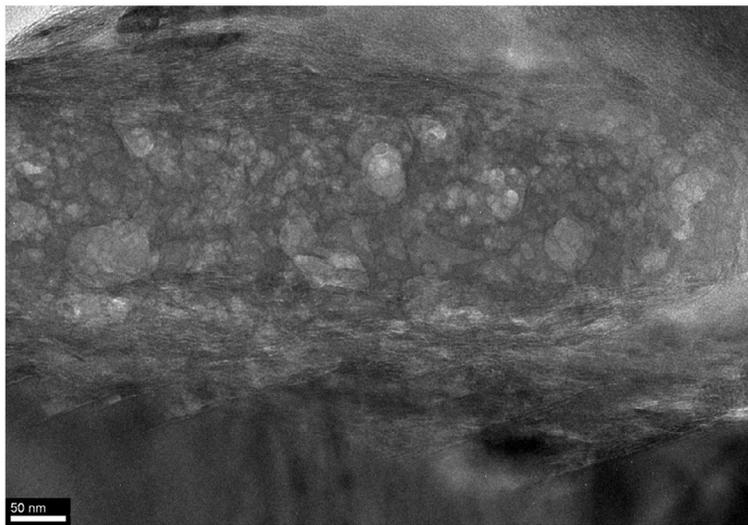
Fig. 27 HRTEM image of silica glaze interdigitating with rock varnish. The dark material at the bottom of the image is the underlying rock. Layered rock varnish forms a 50 nm thick deposit on the underlying rock. The barrier to transport changed, resulting in silica glaze spheroids deposited in a layer about 200 nm thick. Then, layered rock varnish deposited on top of the silica spheroids.
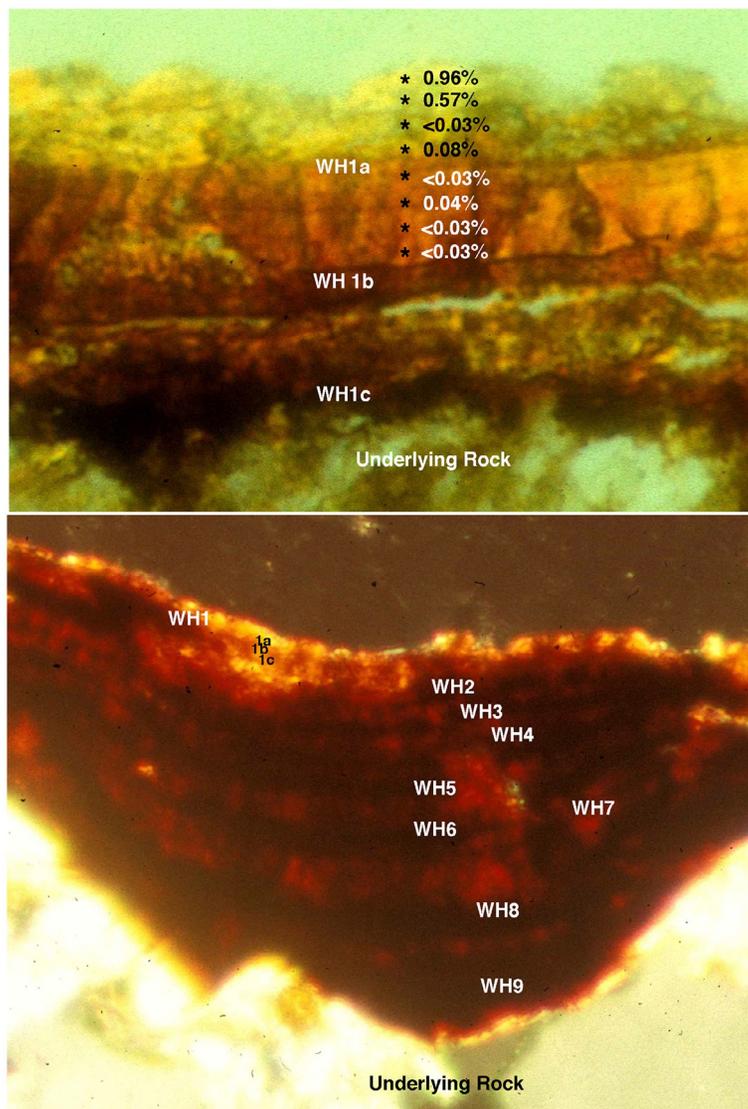
Fig. 28 Microlaminations in rock varnish reflect shifting geochemical barriers. Wetter environments enhance barriers to Mn migration and result in the accretion of dark Mn-rich layers. These ultra-thin sections are of rock varnishes collected from the Ma Ha Tuak Range, Phoenix, Arizona. Wetter microenvironments increase rates of varnishing and can preserve relatively fine paleoclimatic information. The upper section (thickness $\sim$28 μm) shows all three wet phases of the Little Ice Age WH1 signal (Liu and Broecker, 2007): WH1a, WH1b, and WH1c. Also annotated on this section are wavelength dispersive electron microprobe analyses of PbO; these analyses show the typical pattern of lead contamination of the uppermost microns in varnish from 20th century automobile pollution. The values are in PbO weight percent, and the approximate distance between the probe spots are 2 μm. Note how PbO drops down close to or below minimum detection limits underneath this 20th century varnish. The bottom image was collected from a drier microenvironment, and this drier setting slows the rate of varnishing to the point where only the major wet Holocene (WH) periods (Liu and Broecker, 2007) are recorded (thickness $\sim$40 μm).

Fig. 29   Marine Terrace, southern Peru, where up to 4 m of sodium chloride salt crust covers bedrock.

stronger manganese barriers record wet intervals (Liu and Broecker, 2000, 2007, 2013; Broecker and Liu, 2001; Liu et al., 2013, 2021; Carbonelli and Collantes, 2019; Sarmast et al., 2019).

The creation of one geochemical barrier can generate another barrier. Manganese and iron oxides enhanced in rock varnish (Fig. 28) scavenge heavy metals (Jenne, 1968; Thiagarajan and Lee, 2004; Wayne et al., 2006). Modern aerosols are generally much higher in such heavy metals such as lead from the use of leaded gasoline (Ganor et al., 2009). The upper micron in rock varnish, thus, is greatly enhanced in lead, because iron and manganese scavenges this pollutant and fixes it (Fig. 28).

Rock coatings are rarely stable for more than a few thousand years. In a few cases, the layering pattern of varnish microlaminations reveals that stable rock surfaces can host coatings for a few hundred thousand years (Liu and Broecker, 2008b; Liu, 2010). Along the coast of southern Peru, meters of salt crust have coated bedrock of a marine isotope stage 5e marine terrace ($\sim$120,000 years ago) over the last 10^5 years (Fig. 29), and sulfate crusts formed in Victoria Land, Antarctica may be as old as the last time a location was glaciated (Giorgetti and Baroni, 2007). Burial can also preserve rock coatings in Antarctica (Marchant et al., 1996). In one locale, geochemical barriers remained intact after burial, preserving rock varnishes for 10^7 years (Fig. 30) (Dorn and Dickinson, 1989).

An issue that should not be neglected is the role of nucleation sites as important barriers for migration. This is the case for bacteria that concentrate manganese and iron in rock varnish (Fig. 25) (Dorn and Oberlander, 1981; Hungate et al., 1987; Dorn, 2007; Northup et al., 2010). Nucleation sites can also be important in the formation of some sulfate crusts (Fig. 31). Carbon has been observed in weathering rinds extensively in the form of vitrinite and inertinite (Dorn, 1996; Arrowsmith et al., 1996), and its origins could be related to what has been observed in association with plant roots (Sun et al., 2017). Carbon particles are known to serve as sites of gypsum precipitation in urban polluted contexts (Del Monte and Sabbioni, 1984; Del Monte et al., 1984).

In summary, landscape geochemistry theory interprets the presence of rock coatings as reflecting physical, biological, or chemical barriers to the transport of elements. However, the presence of inorganic rock coatings can only occur where there is limited competition from lithobionts such as lichens that can grow much faster. Physical and biogeochemical barriers to transport can be widespread, leading to extensive coatings of rock varnish. These barriers can be linear, resulting in streaks of silica glaze or oxalate crusts. Barriers can also be discrete places, such as carbonate crusts accumulating on the undersides of desert boulders. The geographical expression of such barriers leads to the amazing variety of rock coatings seen in different geomorphic settings.

3   Importance of rock coatings in geomorphology

Rock coatings interface with geomorphology in a variety of ways. At the most general level, the aesthetic and dramatic bare rock landforms that motivate the general public, students and professionals alike are painted by ubiquitous rock coatings. The appearance of favored icons of geomorphology, such as Uluru being coated with iron films (Dorn and Dragovich, 1990) or the spectacular alluvial fans of Death Valley darkened by rock varnish (Dorn, 1988), cannot be separated from landforms. Personal satisfaction associated with field experiences are, thus, inseparably linked with scenic aspects imposed by rock coatings (e.g., Fig. 1).

Rock coatings are also relevant to geomorphological studies, because they can help stabilize landform surfaces through case hardening. Case hardening most often derives from the mobilization and reprecipitation of rock coating materials inside pore
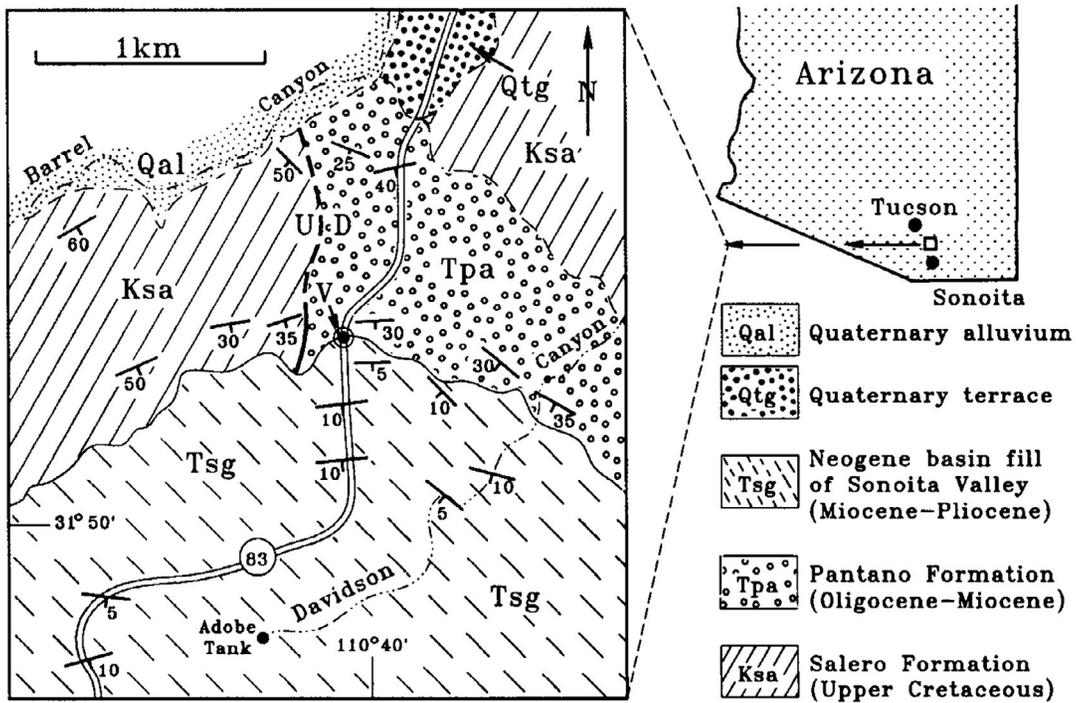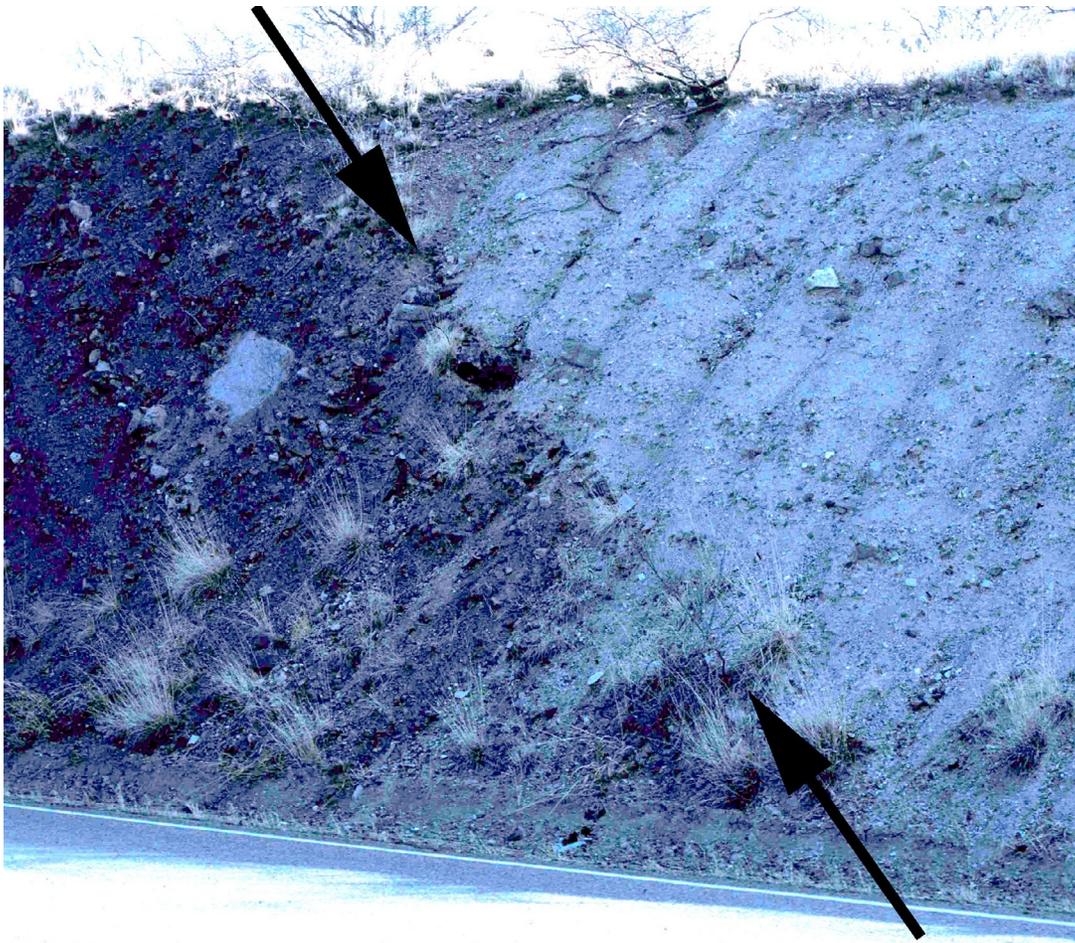
Fig. 30 Rock varnish formed originally on colluvium on a Miocene hillslope of the Pantano Formation has been preserved at Davidson Canyon, southern Arizona, United States. Arrows indicate the varnished colluvial horizon, that is overlain by sandy gravels—part of Neogene basin fill. The composition of this varnish is similar to modern semi-arid varnishes (Dorn and Dickinson, 1989).
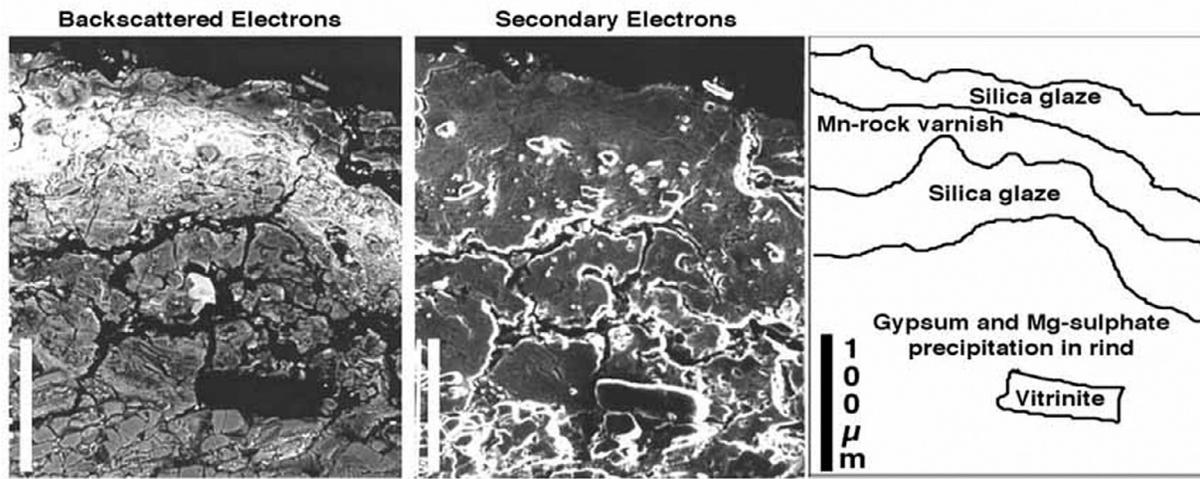
Fig. 31　A particle of vitrinite serves as a nucleation site for sulfate crust precipitation at Karolta, South Australia. This same coal-like material has been observed in association with plant roots (Sun et al., 2017) and could have similar origins. The vitrinite is seen topographically in secondary electrons, but its low atomic number makes it appear dark in back-scattered electrons. After the sulfate crust precipitated around the carbonaceous particle, the landscape geochemistry environment oscillated between favoring silica glaze and rock varnish formation.
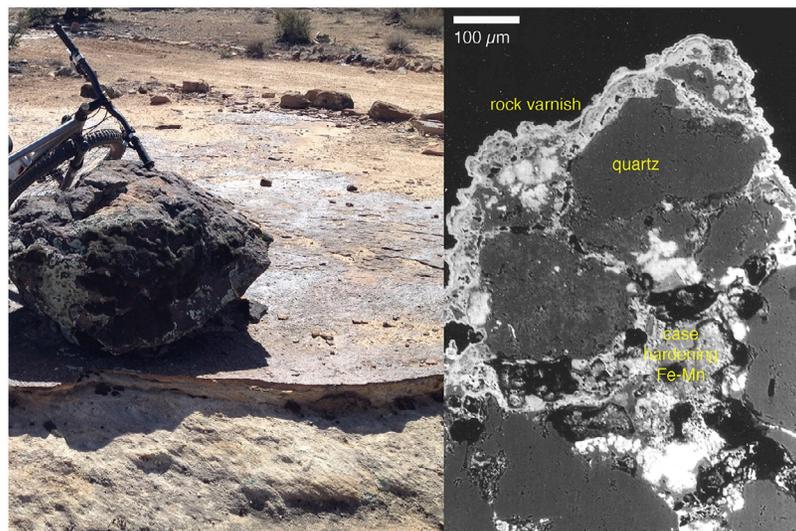
Fig. 32　BSE imagery showing that case hardening occurs from the remobilization of rock coatings into pores in the underlying rock. Left: case hardened surface of sandstone at Gooseberry Mesa, southern Utah, United States. Right: BSE image of rock varnish forming on the sandstone grains, dissolved and reprecipitated inside the pore spaces of the underlying weathering rind. This infilling replaces the original grain-to-grain cement that dissolved to form the weathering rind. The remobilized rock coating materials thus case harden the surface of the sandstone making it more resistant to erosion than the underlying weathering rind.

spaces in the weathering rind (Conca and Rossman, 1982). Calcite is a common mineral that case hardens surfaces (Mellor et al., 1997). Heavy metals also case harden by infilling of pore spaces in a weathering rind, for example sandstone at Petra, Jordan (Fig. 1) and Sedona, Arizona (Fig. 22). Fig. 32 illustrates stabilization of delicate weathering features through reprecipitation of rock varnish and silica glaze. In addition to the migration of single types of coating material into the weathering rinds, different types of mobilized rock coatings are often mixed together inside the weathering rind (Fig. 6).

　　The rock coating material reprecipitated into weathering rinds does more than physically protect through case hardening. In general, chemical weathering rates decrease over time in large part because of the role of clay-coated mineral surfaces (Meunier et al., 2007). Some types of rock coatings, such as silica glaze, can slow the rate of chemical weathering (Gordon and Dorn, 2005b). In a study of basalt surfaces of known age in Hawaii, chemical dissolution of plagiocase under silica glaze was much lower than plagioclase not covered by silica glaze (Table 2).

Table 2   Weathering of plagioclase[a] grains of Hawaiian basalt surfaces exposed for different lengths of time, underneath silica glaze and not under silica glaze.

Surface	Not Under Silica Glaze		Under Silica Glaze	
	Grain Area[b]	Porosity[c]	Grain Area[b]	Porosity[c]
Mauna Ulu-a (1974 C.E.)	217,500	0.071 ± 0.018	160,500	0.009 ± 0.018
Mauna Ulu-b (1974 C.E.)	216,000	0.058 ± 0.014	216,500	0.008 ± 0.011
Mauna Ulu-c (1974 C.E.)	202,500	0.007 ± 0.004	247,000	0.010 ± 0.022
Flow f7d h7.9 (~700 B.P.)	238,500	0.94 ± 0.17	183,500	0.13 ± 0.19
Flow f5d c8.2 (~2000 B.P.)	303,000	1.63 ± 0.15	160,500	0.39 ± 0.23
Flow f5d p3.5 (~3150 B.P.)	141,000	2.90 ± 0.25	185,500	0.54 ± 0.33
Mauna Kea Glacial Polish (~14,000 B.P.)	201,500	26.20 ± 10.33	154,000	15.71 ± 5.82

[a]Representative composition in oxide weight percent of analyzed plagioclase minerals: 3.22% Na_2O, 0.22% MgO, 29.12% Al_2O_3, 48.22% SiO_2, 18.10% CaO, 0.12% TiO_2, 0.40% MnO, and 0.54% FeO.
[b]Grain area is measured in square micrometers as a total for all mineral grains analyzed.
[c]Each value indicates the average and standard deviation of the porosity measurements.

Other types of rock coatings can, in contradistinction, accelerate the physical weathering of rocks. The calcrete crust and dust films that precipitate and accumulate inside rock fissures (Fig. 4) wedge open those fractures (Coudé-Gaussen et al., 1984; Villa et al., 1995; Cerveny et al., 2006; Dorn et al., 2008) in a process called dirt cracking (Dorn, 2011). Dirt cracking is the most quantitatively significant physical weathering process yet known to occur in warm desert settings (Dorn, 2018).

The study of rock coatings includes an extensive effort to use characteristics of these coatings to determine exposure age. This aspect of rock coating research is often an attraction to researchers who are just starting to explore coatings (Li et al., 2019). In particular, rock varnish has seen decades of study in order to determine if different characteristics could be used to assess when varnish started to form. Knowing the approximate starting time for varnishing would, therefore, provide insight into the age of a glacial moraine, alluvial-fan deposit, stream terrace, landslide, or other feature. Table 3 presents the various strategies that have been proposed to estimate the start of varnishing and hence provide a minimum chronomety for exposure of the underlying surface.

Out of these different dating methods, I believe that the most advanced approach is the result of a quarter-century of research by Tanzhuo Liu of Columbia University. Scholarly research into rock coating initiated with the field and laboratory studies of rock varnish by Alexander von Humboldt (von Humboldt, 1812). Rock coating studies over the past two centuries have typically focused on a handful of samples. In contrast, Dr. Liu has analyzed more than 10,000 microstratigraphic sequences of rock varnishes obtained from millimeter-scale rock depressions (e.g., Fig. 33). His painstaking analysis of varnishes, based on the study of three orders of magnitude more samples than analyzed in a typical publication, has led to a revolution in our understanding of how climatic changes are recorded by varnish microlaminations (Liu and Broecker, 2007, 2008a,b, 2013; Liu, 2010; Liu et al., 2013). The confidence level is high, because the method (Liu, 2003; Liu and Broecker, 2007) has been replicated in a rigorous blind test (Marston, 2003), the method is based on analyses of over ten thousand rock microbasins (Liu and Broecker, 2008a, 2013; Liu et al., 2013), is supported by nanoscale analyses (Krinsley et al., 2013), and has been used by a variety of researchers (Zerboni, 2008; Somonte and Baied, 2013; Dorn, 2018; Carbonelli and Collantes, 2019).

A leading authority in the area of applied geomorphic research on analyzing signals of pollution on rock coatings is Dr. Michael Schindler, who with co-authors, has detailed the processes and forms linking anthropogenic heavy metal pollution to the anthropogenic rock coatings (Durocher and Schindler, 2011; Mantha et al., 2012, 2019; Schindler et al., 2017; Schindler and Dorn, 2017; Schindler and Singer, 2017; Caplette and Schindler, 2018; Leverington and Schindler, 2018). Natural rock coatings such as iron films and rock varnish are also impacted by anthropogenic heavy metal pollution. Even in regions as remote as Greenland, the global effect of lead pollution leaves an Anthropocene signal (Fig. 34). This lead signature (Fleisher et al., 1999; Nowinski et al., 2010; Hoar et al., 2011; Spilde et al., 2013) was originally used as a way to falsify a fake geoglyph (Dorn, 1998). The lead spike in iron films and rock varnish, along with the varnish microlamination method (Table 3) has also been used as a process to authenticate (or assess fake) prehistoric engravings (Dorn et al., 2012b).

Even though this chapter focuses on terrestrial settings, rock coatings occur in extraterrestrial contexts, such as the ubiquitous dust coatings on lunar surfaces (Gaier, 2005). The discovery of Mn-rich rock coatings on Mars (Lanza et al., 2014a,b, 2015) naturally led to comparisons with rock varnish in terrestrial settings (Yeager et al., 2019). With experience of over 40 years of publications on terrestrial rock varnish, I have examined thousands of images acquired by different rovers operating on the surface of Mars. The

Table 3   Different methods that have been used to assess rock varnish chronometry.

Method	Synopsis of method
^{14}C carbonate	Calcium carbonate sometimes forms over varnish, and can be radiocarbon dated, providing a minimum age for such features as rock art. The method has been used in Australia (Dragovich, 1986) and eastern California (Smith and Turner, 1975; Cerveny et al., 2006).
^{14}C organic	The hope is that carbon trapped by coating provides minimum age for the petroglyph. First developed in 1986, two independent investigators working in a blind test (Dorn, 1997; Watchman, 1997) both found organic carbon that pre-dates and post-dates the exposure of the rock surface. The only person who still uses organic carbon of unknown residues in radiocarbon dating (Watchman, 2000; Huyge et al., 2001), Watchman now admits that he has not tested results against independent controls (Watchman, 2002; Whitley and Simon, 2002a,b).
^{14}C oxalate	The inorganic mineral oxalate (e.g., whewellite: $CaC_2O_4 \bullet H_2O$) sometimes deposits on top of or underneath rock varnish (Watchman et al., 2000). Because this mineral contains datable carbon, the radiocarbon age can provide a minimum age for the underlying or overlying varnish. The most reliable research on radiocarbon dating of oxalates in rock surface contexts has been conducted in west Texas (Rowe, 2001; Spades and Russ, 2005).
Accumulation of Mn and Fe	As more varnish accumulates, the mass of manganese and iron gradually increases. Occasionally this old idea is resurrected (Lytle et al., 2002), most recently in petroglyph research in Saudi Arabia where so many different variables other than time influence Mn and Fe abundance that the method is impractical for general use and requires extraordinary effort to make this approach workable (Macholdt et al., 2019), and sometimes it does not work (Andreae et al., 2020). Without extensive assumptions and costly research, this approach has long ago been demonstrated to yield inaccurate results in tests against independent control (Bard, 1979; Dorn, 2001).
Appearance	The appearance of a surface darkens over time as varnish thickens and increases in coverage (McFadden et al., 1989). However, much of this darkening has to do with exposure of inherited coatings, and with the nature of the underlying weathering rinds, that do not permit accurate or precise assignment of ages based on visual appearance. There is no known visual method that yields reliable and replicable results.
Cation-ratio dating	Rock varnish contains elements that are leached (washed out) rapidly (Dorn and Krinsley, 1991; Krinsley, 1998). Over time, a ratio of leached to immobile elements decline over time (Dorn, 2001). If the correct type of varnish is used, the method performs well in blind tests (Loendorf, 1991). This method has also seen use in such places as China (Zhang et al., 1990), Israel (Patyk-Kara et al., 1997), and South Africa (Whitley and Annegarn, 1994), Yemen (Harrington, 1986), Iran (Sarmast et al., 2017) and elsewhere (Ntokos, 2021).
Foreign Material Analysis	Rock carvings made historically may have used steel. The presence of steel remains embedded in a carving would invalidate claims of antiquity, whereas presence of such material as quartz would be consistent with prehistoric antiquity (Whitley et al., 1999).
Lead Profiles	20th century lead and other metal pollution is recorded in rock varnish, because the iron and manganese in varnish scavenges lead and other metals. This leads to a "spike" in the very surface micron from 20th century pollution. Confidence is reasonably high, because the method (Dorn, 1998, pp. 139) has been replicated (Fleisher et al., 1999; Thiagarajan and Lee, 2004; Hodge et al., 2005) with no publications yet critical of the technique that can discriminate 20th century from pre-20th century surfaces.
Microoaminations (VML)	Climate fluctuations change the pattern of varnish microlaminations (VML). The method must be calibrated by numerical ages, and this is typically done using a combination of different methods to establish independent chronologies. The geomorphological implications this method (Liu, 2021) are profound, offering desert geomorphologists a tool to study in tandem chronometry and the influence of climatic change.
Organic Carbon Ratio	Organic carbon exists in an open system in the rock varnish that covers petroglyphs. This method compares the more mobile carbon and the more stable carbon. The method is best used in soil settings (Harrison and Frink, 2000), but it has been applied experimentally to rock varnish in desert pavements (Dorn et al., 2001).
Uranium-series dating	Since radionuclides are enhanced in varnish (Marshall, 1962), uranium-series isotopes show potential (Knauss and Ku, 1980). Complications surround acquiring the necessary amount of material from the basal layers and concerns over accounting for the abundant thorium that derives from clay detritus instead of radioactive decay.

study of geomorphology on Mars is not my area of expertise, and I am reluctant to analyze processes operating under vastly different physical and chemical conditions. Taken purely from a terrestrial perspective, however, I have seen no clear evidence of active varnish formation on subaerial rock surfaces on Mars, although there are some images that are suggestive of subaerial varnish formation. The reason for my scepticism is that I see overwhelming evidence of aeolian abrasion that appears to be removing dark rock coatings. I think that the Mn-rich coatings on the surface of Mars likely originated in rock fractures (Krinsley et al., 2009). Please re-examine Figs. 4 and 5 in this chapter. The rock fractures do not have to be deep. They can be centimeters under the surface, but protected from aeolian abrasion and potentially providing a biogeochemical setting able to develop a varnish-like coating. Then, spalling of the overlying rock material exposesrock coatings to the subaerial Mars environment.

Although Mn-rich coatings do occur on Mars (Lanza et al., 2014a,b, 2015), Dorn (1998) predicted that silica glazes should be more common on Mars, and silica glazes in terrestrial volcanic settings have been investigated as potential analogs (Minitti et al., 2005, 2007; Chemtob et al., 2010; Chemtob and Rossman, 2014). An analysis of chemical weathering conditions on Mars (Kraft et al., 2004) suggests that four steps might be involved in the formation of silica glazes on Mars: (a) a fresh rock surface is exposed; (b) dust is deposited on rock surfaces; (c) "thin films of liquid water form between dust grains along the dust-rock interface" leading to (d) silica glaze deposition (Kraft et al., 2004).

There is another possibility to explain the possible occurrence of silica glaze on Mars and Earth that has not yet been considered in Mars rock coating scholarship: water vapor. An unsolved problem on the geography of terrestrial rock coatings concerns why rock
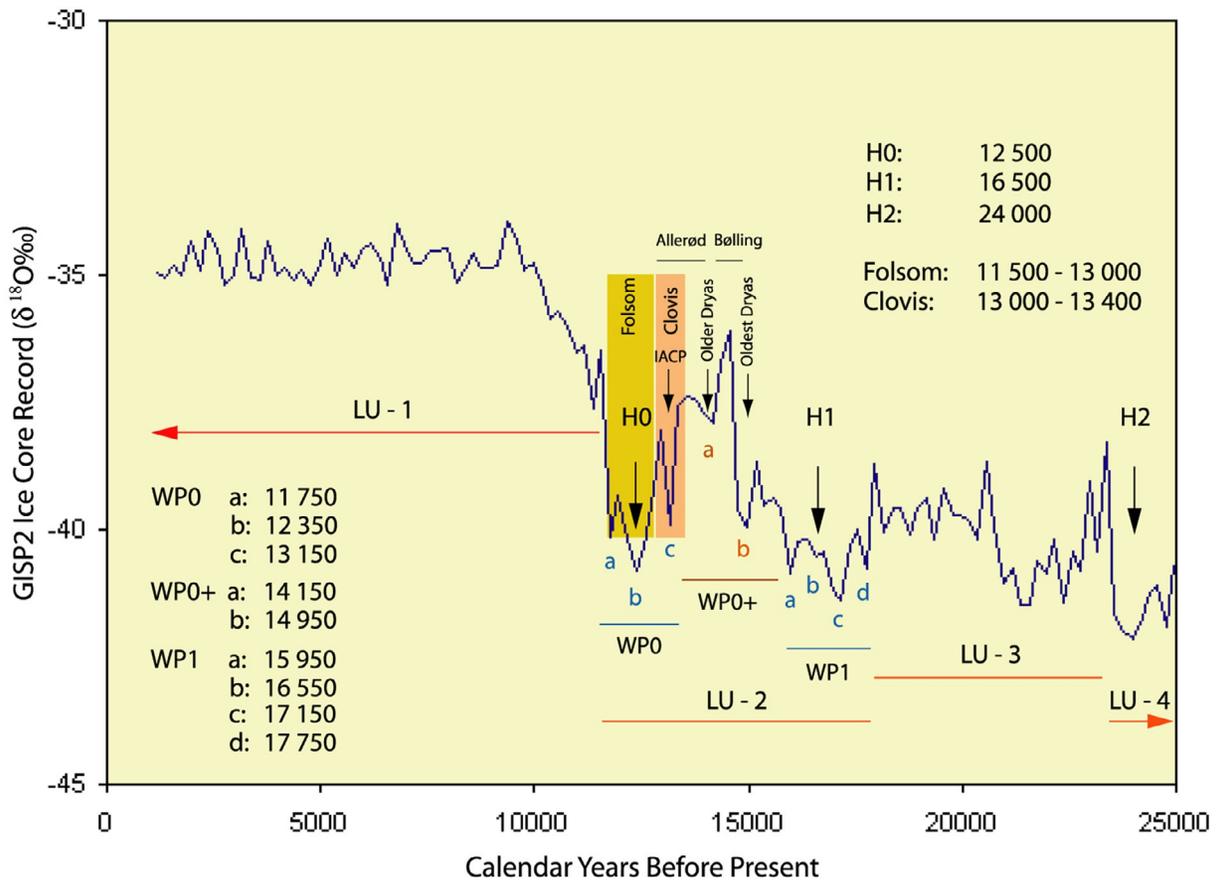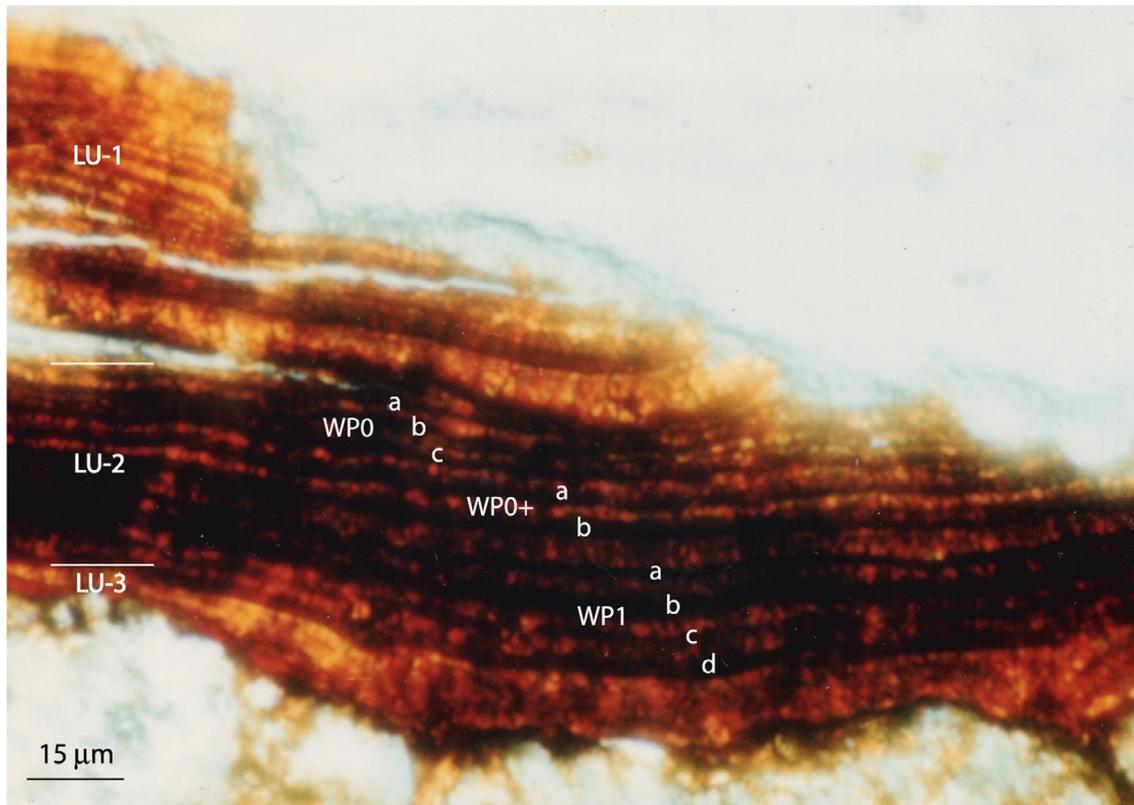
Fig. 33 A varnish ultra-thin section from Galena Canyon fan in Death Valley (with the upper layers irregularly polished off during thin section production) exemplifies a terminal Pleistocene varnish microlamination pattern. The age correlation presented here comes from independent numerical age control and from the Greenland ice core record. For the sake of temporal recognition, the well-known Folsom and Clovis lithic technologies are placed in this high resolution sequence. The nomenclature of layering units (LU), Heinrich Events (e.g., H0, H1, H2), wet periods in the late Pleistocene (WP) identified by black varnish layers follows previous research (Liu and Broecker, 2007, 2008a,b; Liu, 2010). The image is courtesy of T. Liu.
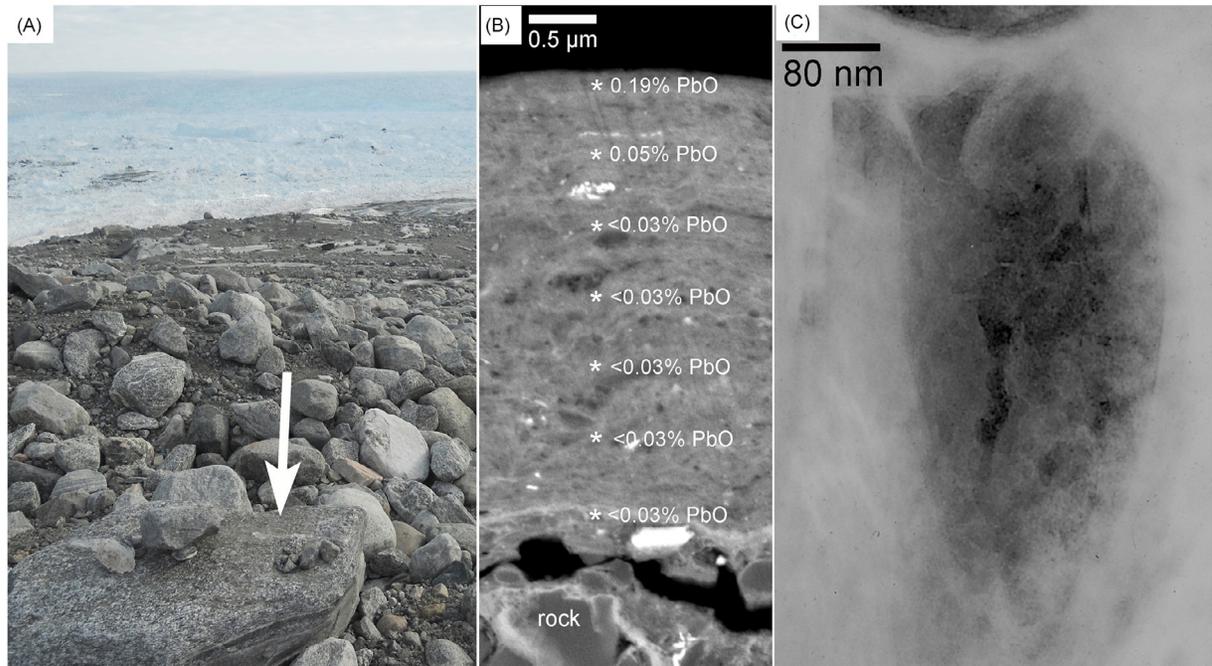
Fig. 34   Anthropogenic lead emissions contaminate the surfaces of rock coatings even in areas distant from emission sources. (A) Gneissic boulder on the edge of a Greenland outlet glacier, where the white arrow indicates the sampling location of a pocket of Mn-rich rock varnish. (B) Mn-rich rock varnish identifying the locations of wavelength dispersive microprobe analyses for lead where <0.03% PbO is the background level. Note that the surface-most analysis contains 0.19% PbO. (C) Nanoscale HRTEM image of the location of the high lead measurement. The dark material is Mn-rich material, where the darkest zones have EDX peaks indicative of lead.

varnish is so common in subtropical deserts, but silica glaze is ubiquitous on basalt surfaces in rainshadows of Hawaiian volcanoes Haleakala, Mauna Loa, Mauna Kea, and Hualalai. One possible explanation is that the paucity of dust inhibits varnish formation that is dependent on clay minerals. However, the abundance of water vapor in this tropical context could not be ruled out. Thus, a 20 year laboratory experiment exposed basalt rock chips to 80% and 90% levels of relative humidity. No liquid water was involved. This experiment found that water vapor alone can generate silica glaze (Dorn, 2012) and may be an important factor in explaining why silica glaze is the dominant rock coating in humid warm drylands (Fig. 35). Although water vapor concentrations on Mars are
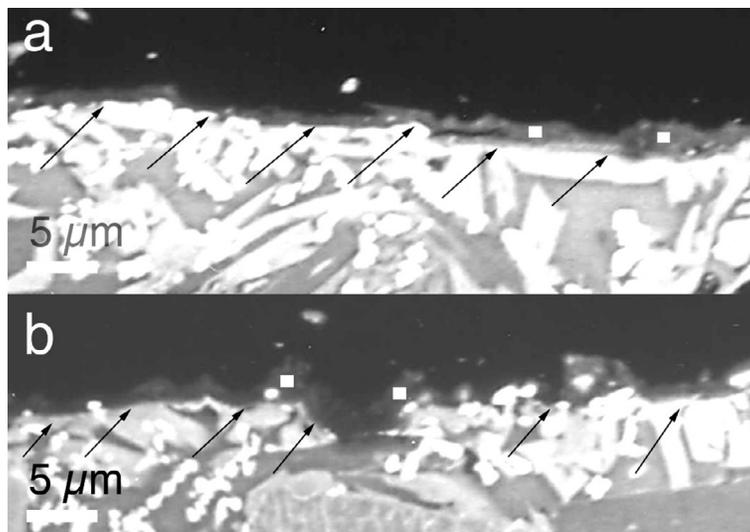
Fig. 35   BSE images of silica glaze formed on basalt rock chips after exposure to only air with a relative humidity of (A) 90% and (B) 80% at 18 °C in a 20-year-long laboratory experiment. Arrows show contacts between the silica glaze and the underlying basalt. The white dots indicate the positions of focused beam electron microprobe measurements. A typical water vapor-formed silica glaze composition is MgO 0.06%, Al_2O_3 0.57%, 80.22% SiO_2, 0.04% K_2O, 0.22% CaO, 0.08% TiO_2, 0.06% Fe_2O_3 with abundant porosity.

extremely small, the length of time for mineral—water vapor interactions on Mars make it possible that coatings of amorphous silica found on Mars could be a product of billions of years of nanoscale water vapor interaction.

4 Conclusion

The first formal scholarship on rock coatings (von Humboldt, 1812) advocated for the hypothesis that the blackened rocks along the Orinoco River are Mn-enriched accretions on the underlying rock. A revisitation of von Humboldt's coatings over two centuries later (Dorn et al., 2012c) confirmed their accretionary nature (Fig. 36). Prior to the late 1970s, however, the dominant view of rock coatings were that they derived from the weathered products of the underlying rock (Dorn, 1998); this "from the rock" paradigm was overwhelmingly falsified by secondary electron microscopy images (Potter and Rossman, 1977), delicately made ultra-thin cross-sections (Perry and Adams, 1978), and the first high resolution transmission electron microscope images (Krinsley et al., 1995). The academic debate over the internal vs. external origin of varnish constituents sometimes still emerges when investigators fail to use what are now basic tools in electron microscopy, but the reality is that the direction of material flow is actually the opposite of what was thought throughout much of the 20th century. Dissolution of rock coating accretions results in the translocation of externally-applied materials downward into the rock to produce case hardening (Dorn et al., 2012a, 2017) of weathering rinds (Fig. 32).

   Rock varnish is but one of fourteen different types of coatings that cover rocks in the terrestrial weathering environment. Some coatings are always found separately, while others blend together creating an almost infinite variety. The only general theory that has been proposed to understand rock coatings is the paradigm of landscape geochemistry, originally developed by Soviet geographers. This framework focuses on the spatial aspects of biogeochemistry and interprets rock coatings in terms of element abundance, element migration, geochemical flows, geochemical gradients, and geochemical barriers. These components of understanding rock coatings are reorganized here in a hierarchy of five orders of control on what types of rock coatings develop:

- *1st order*: bare rock faces must be exposed by erosional processes for rock coatings to be seen
- *2nd order*: coatings originally formed in the subsurface can be exposed by erosional processes and are inherited from a different landscape geochemistry environment
- *3rd order*: lithobionts such as lichens dominate rock surfaces in conditions where they grow much faster than inorganic rock coatings
- *4th order*: the elements of rock coatings must be transported to bare rock surfaces;
- *5th order*: barriers to the further transport of constituents result in the accumulation of rock coatings.

Rock coatings are important to the broader field of geomorphology in several different ways. They alter the appearance of bedrock landforms. Coatings can promote surface stability through case hardening; this first involves the mobilization of constituents from rock coatings and then reprecipitation within the pore spaces of the underlying weathering rind. In contrast, rock coatings formed in rock fissures in dusty warm deserts can accelerate physical weathering rates substantially through wedging rocks apart. Rock coatings likely occur as silica glaze on Mars. One of the most significant aspects of rock coatings in geomorphology rests with the revolutionary research by Tanzhuo Liu, where two decades of painstaking analysis of over 10,000 microsedimentary basins exemplifies how rock coatings can be used to analyze paleoclimatic changes and also provide minimum ages to understand landform evolution.
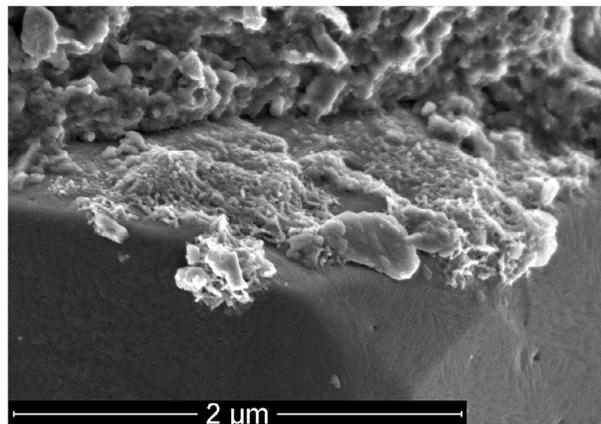

Fig. 36 Secondary electron image of rock varnish of von Humboldt's (1812) Orinoco site of rock varnish formed on quartz. Even at the scale where the coating is less than 100 nm thin, the accretionary nature of rock varnish is dramatically apparent.

Acknowledgment

References

Aftabi A and Atapour H (2018) A new record of silica-rich coating on carbonate substrates in southeast-central Iran: Constraints on geochemical signatures. *Sedimentary Geology* 372: 64–74.

Aghamiri R and Schwartzman DW (2002) Weathering rates of bedrock by lichens: A mini watershed study. *Chemical Geology* 188: 249–259.

Andreae MO, Al-Amri A, Andreae TW, Garfinkel A, Haug G, Jochum KP, Stoll B, and Weis U (2020) Geochemical studies on rock varnish and petroglyphs in the Owens and Rose valleys, California. *PLoS One* 15(8): e0235421. https://doi.org/10.1371/journal.pone.0235421.

Arocena JM and Hall K (2003) Calcium phosphate coatings on the Yalour Islands, Antarctica: Formation and geomorphic implication. *Arctic Antarctic and Alpine Research* 35: 233–241.

Arp G, Thiel V, Reimer A, Michaelis W, and Reitner J (1999) Biofilm expolymers control microbialite formation at thermal springs discharging into the alkaline pyramid lake, Nevada, USA. *Sedimentary Geology* 126: 159–176.

Arrowsmith JR, Rice GE and Hower JC (1996) *Documentation of carbon-rich fragments in varnish-covered rocks from Central Arizona using electron microscopy and coal petrography*. Submitted to Science.

Bard JC (1979) *The Development of a Patination Dating Technique for Great Basin Petroglyphs Utilizing Neutron Activation and X-Ray Fluorescence Analyses*. Ph.D. Dissertation Berkeley: University of California 409.

Benson L (1994) Carbonate deposition, pyramid lake subbasin, Nevada: 1. Sequence of formation and elevational distribution of carbonate deposits (tufas). *Palaeogeography, Palaeoclimatology, Palaeoecology* 109: 55–87.

Benson LV, Hattori EM, Southon JR, and Aleck B (2013) Dating North America's oldest petroglyphs, Winnemucca lake subbasin, Nevada. *Journal of Archaeological Science* 40: 4466–4476.

Benzerara K, Chapon V, Moreira D, Lopez-Garcia P, Guyot F, and Heulin T (2006) Microbial diversity on the Tatahouine meteorite. *Meteoritics & Planetary Science* 41: 1259–1265.

Berger JA, Kin PL, Green A, Craig MA, Spilde MN, Wright SO, Kunkel TS, and Lee RJ (2015) Effect of halite coatings on thermal infrared spectra. *Journal of Geophysical Research. Solid Earth* 120: 2162–2178.

Bhatnagar A and Bhatnagar M (2005) Microbial diversity in desert ecosystems. *Current Science* 89: 91–100.

Bishop JL, Murchie SL, Pieters CM, and Zent AP (2002) A model for formation of dust, soil, and rock coatings on Mars: Physical and chemical processes on the Martian surface. *Journal of Geophysical Research* 107(E11). https://doi.org/10.1029/2001JE001581.

Blake WP (1905) Superficial blackening and discoloration of rocks especially in desert regions. *Transactions of the American Institute of Mining Engineers* 35: 371–375.

Boston PJ, Spilde MN, Northup DE, and Dichosa A (2008) Biogenic Fe/Mn oxides in caves and surface desert varnish: Potential biosignatures for earth and mars. *Astrobiology* 8: 448.

Brewer TE and Fierer N (2018) Tales from the tomb: The microbial ecology of exposed rock surfaces. *Environmental Microbiology* 20: 958–970.

Broecker WS and Liu T (2001) Rock varnish: Recorder of desert wetness? *GSA Today* 11(8): 4–10.

Browne BA and Driscoll CT (1992) Soluble aluminum silicates: Stoichiometry, stability, and implications for environmental geochemistry. *Science* 256: 1667–1669.

Camuffo D, Del Monte M, and Sabbioni C (1983) Origin and growth mechanisms of the sulfated crusts on urban limestone. *Water, Air and Solution Pollution* 19: 351–359.

Caplette JN and Schindler M (2018) Black rock-coatings in trail, British Columbia, Canada: Records of past emissions of lead, zinc, antimony, arsenic, tellurium, tin, selenium, silver, bismuth, and indium-bearing atmospheric contaminants. *The Canadian Mineralogist* 56: 113–127.

Carbonelli JP and Collantes MM (2019) *Early Human Occupations in the Valleys of Northwestern Argentina: Contributions to Dating by the Varnish Micro-Laminations Technique Advances in Geomorphology and Quaternary Studies in Argentina*. Amsterdam: Springer 262–282.

Carter CL, Dethier DP, and Newton RL (2003) Subglacial environment inferred from bedrock-coating siltskins, Mendenhall Glacier, Alaska, USA. *Journal of Glaciology* 49: 568–576.

Cerveny NV, Kaldenberg R, Reed J, Whitley DS, Simon J, and Dorn RI (2006) A new strategy for analyzing the chronometry of constructed rock features in deserts. *Geoarchaeology* 21: 181–203.

Chemtob SM and Rossman GR (2014) Timescales and mechanisms of formation of amorphous silica coatings on fresh basalts at Kīlauea Volcano, Hawai'i. *Journal of Volcanology and Geothermal Research* 286: 41–54.

Chemtob SM, Jolliff BL, Rossman GR, Eiler JM, and Arvidson RE (2010) Silica coatings in the Ka'u desert, Hawaii, a Mars analog terriain: A micromorphological, spectral, chemical and isotopic study. *Journal of Geophysical Research* 115(E04001). https://doi.org/10.1029/2009JE003473.

Churaev NV (2003) Surface forces in wetting films. *Advances in Colloid and Interface Science* 103: 197–218.

Conca JL and Rossman GR (1982) Case hardening of sandstone. *Geology* 10: 520–525.

Coudé-Gaussen G, Rognon P, and Federoff N (1984) Piegeage de poussières éoliennes dans des fissures de granitoides due Sinai oriental. *Compte Rendus de l'Academie des Sciences de Paris II* 298: 369–374.

Del Monte M and Sabbioni C (1984) Gypsum crusts and fly ash particles on carbonate outcrops. *Archives for Meteorology, Geophysics and Bioclimatology Series B* 35: 105–111.

Del Monte M, Sabbioni C, Ventura A, and Zappia G (1984) Crystal growth from carbonaceous particles. *The Science of the Total Environment* 36: 247–254.

Donoghue E, Troll VR, Schwarzkopf LM, Clayton G, and Goodhue R (2009) Organic block coatings in block-and-ash flow deposits at Merapi volcano, Central Java. *Geological Magazine* 146: 113–120.

Dorn RI (1988) A rock varnish interpretation of alluvial-fan development in Death Valley, California. *National Geographic Research* 4: 56–73.

Dorn RI (1996) Uncertainties in ^{14}C ages for petroglyphs from the Olary province, South Australia. *Archaeology in Oceania* 31: 214–215.

Dorn RI (1997) Constraining the age of the Côa valley (Portugal) engravings with radiocarbon dating. *Antiquity* 71: 105–115.

Dorn RI (1998) *Rock Coatings*. Amsterdam: Elsevier 429.

Dorn RI (2001) Chronometric techniques: Engravings. In: Whitley DS (ed.) *Handbook of Rock Art Research*, pp. 167–189. Walnut Creek: Altamira Press.

Dorn RI (2007) Rock varnish. In: Nash DJ and McLaren SJ (eds.) *Geochemical Sediments and Landscapes*, pp. 246–297. London: Blackwell.

Dorn RI (2011) Revisiting dirt cracking as a physical weathering process in warm deserts. *Geomorphology* 135: 129–142.

Dorn RI (2012) Formation of silica glaze rock coatings through water vapor interactions. *Physical Geography* 33: 21–31.

Dorn RI (2018) Necrogeomorphology and the life expectancy of desert bedrock landforms. *Progress in Physical Geography* 82: 566–587.

Dorn RI and Dickinson WR (1989) First paleoenvironmental interpretation of a pre-quaternary rock varnish site, Davidson Canyon, South Arizona. *Geology* 17: 1029–1031.

Dorn RI and Dragovich D (1990) Interpretation of rock varnish in Australia: Case studies from the arid zone. *Australian Geographer* 21: 18–32.

Dorn RI and Krinsley DH (1991) Cation-leaching sites in rock varnish. *Geology* 19: 1077–1080.

Dorn RI and Krinsley DH (2011) Spatial, temporal and geographic considerations of the problem of rock varnish diagenesis. *Geomorphology* 130: 91–99.

Dorn RI and Meek N (1995) Rapid formation of rock varnish and other rock coatings on slag deposits near Fontana. *Earth Surface Processes and Landforms* 20: 547–560.

Dorn RI and Oberlander TM (1981) Microbial origin of desert varnish. *Science* 213: 1245–1247.

Dorn RI and Oberlander TM (1982) Rock varnish. *Progress in Physical Geography* 6: 317–367.

Dorn RI, Stasack E, Stasack D, and Clarkson P (2001) Through the looking glass: Analyzing petroglyphs and geoglyphs with different perspectives. *American Indian Rock Art* 27: 77–96.

Dorn RI, Whitley DS, Cerveny NC, Gordon SJ, Allen C, and Gutbrod E (2008) The rock art stability index: A new strategy for maximizing the sustainability of rock art as a heritage resource. *Heritage Management* 1: 35–70.

Dorn RI, Dorn J, Harrison E, Gutbrod E, Gibson S, Larson P, Cerveny N, Lopat N, Groom KM, and Allen CD (2012a) Case hardening vignettes from the western USA: Convergence of form as a result of divergent hardening processes. *Yearbook of the Association of Pacific Coast Geographers* 74: 1–12.

Dorn RI, Gordon M, Pagán EO, Bostwick TW, King M, and Ostapuk P (2012b) Assessing early Spanish explorer routes through authentication of rock inscriptions. *The Professional Geographer* 64: 415–429.

Dorn RI, Krinsley DH, and Ditto J (2012c) Alexander von Humbodlt's initiation of rock coating research. *Journal of Geology* 120: 1–12.

Dorn RI, Mahaney WC, and Krinsley DH (2017) Case hardening: Turning weathering rinds into protective shells. *Elements* 13: 155–158.

Douglas GR (1987) Manganese-rich rock coatings from Iceland. *Earth Surface Processes and Landforms* 12: 301–310.

Dragovich D (1986) Minimum age of some desert varnish near Broken Hill, New South Wales. *Search* 17: 149–151.

Dragovich D (1987) Weathering of desert varnish by lichens. In: Conacher A (ed.) *Readings in Australian Geography. Proceedings of the 21st IAG Conference, Perth* 407–412.

Durocher JL and Schindler M (2011) Iron-hydroxide, iron-sulfate and hydrous-silica coatings in acid-mine tailings facilities: A comparative study of their trace-element composition. *Applied Geochemistry* 26: 1337–1352.

Ehlen J and Wohl E (2002) Joints and landform evolution in bedrock canyons. *Transactions of the Japanese Geomorphological Union* 23(2): 237–255.

Engel CG and Sharp RS (1958) Chemical data on desert varnish. *Geological Society of America Bulletin* 69: 487–518.

Eppard M, Krumbein WE, Koch C, Rhiel E, Staley JT, and Stackebrandt E (1996) Morphological, physiological, and molecular characterization of actinomycetes isolated from dry soil, rocks, and monument surfaces. *Archives of Microbiology* 166: 12–22.

Esposito A, Ahmed E, Cizzazzo S, Skorski J, Overmann J, Holmstrom SJM, and Brusetti L (2015) Comparison of rock varnish bacterial communities with surrounding non-varnished rock surfaces: Taxon-specific analysis and morphological description. *Microbial Ecology* 70: 741–750.

Esposito A, Borruso L, Rattray JE, Brusetti L, and Ahmed E (2019) Taxonomic and functional insights into rock varnish microbiome using shotgun metagenomics. *FEMS Microbiology Ecology* 95. https://doi.org/10.1093/femsec/fiz180.

Fleisher M, Liu T, Broecker W, and Moore W (1999) A clue regarding the origin of rock varnish. *Geophysical Research Letters* 26(1): 103–106.

Fortescue JAC (1980) *Environmental Geochemistry. A Holistic Approach*. New York: Springer-Verlag 347.

Frazier CS and Graham RC (2000) Pedogenic transformation of fractured granitic bedrock, southern California. *Soil Science Society of America Journal* 64: 2057–2069.

Friedmann EI and Galun M (1974) *Desert Algae, Lichen, and Fungi*. New York: Academic Press 165–212.

Gadd GM (2007) Geomycrology: Biogeochemical transformations of rocks, minerals, metals and radionuclides by fungi, bioweathering and bioremediation. *Mycological Research* 111: 3–49.

Gadd GM (2017) Fungi, rocks, and minerals. *Elements* 13: 171–176.

Gaier JR (2005) *The Effects of Lunar Dust on EVA Systems During the Apollo Missions*. NASA/TM—2005-213610 Hanover, Maryland: NASA Center for Aerospace Information 66.

Gallach X, Perrette Y, Lafon D, Chalmin É, Deline P, Ravanel L, Carcaillet J, and Wallet T (2021) A new method for dating the surface exposure age of granite rock walls in the Mont Blanc massif by reflectance spectroscopy. *Quaternary Geochronology* 64: 101156. https://doi.org/10.1016/j.quageo.2021.101156.

Gallinaro M and Zerboni A (2021) Rock, pigments, and weathering. A preliminary assessment of the challenges and potential of physical and biochemical studies on rock art from southern Ethiopia. *Quaternary International* 572: 41–51.

Ganor E, Kronfeld J, Feldman HR, Rosenfeld A, and Ilani S (2009) Environmental dust: A tool to study the patina of ancient artifacts. *Journal of Arid Environments* 73: 1170–1176.

Gaylarde C, Ogawa A, Beech I, Kowalski M, and Baptista-Neto JA (2017) Analysis of dark crusts on the church of Nossa Senhora do Carmo in Rio de Janeiro, Brazil, using chemical, microscope and metabarcoding microbial identification techniques. *International Biodeterioration & Biodegradation* 317: 60–67.

Gazquez F, Calaforra JM, and Forti P (2011) Black Mn-Fe crusts as markers of abrupt palaeoenvironmental changes in El Soplao Cave (Cantabria, Spain). *International Journal of Speleology* 40: 163–169.

Gazquez F, Calaforra JM, and Rull F (2012) Boxwork and ferromanganese coatings in hypogenic caves: An example from Sima de la Higuera Cave (Murcia, SE Spain). *Geomorphology* 177-178: 158–166.

Gázquez F, Calaforra JM, and Rull F (2012) Boxwork and ferromanganese coatings in hypogenic caves: An example from Sima de la Higuera Cave (Murcia, SE Spain). *Geomorphology* 177: 158–166.

Gehrmann C, Krumbein WE, and Petersen K (1988) Lichen weathering activities on mineral and rock surfaces. *Studia Geobotanica* 8: 33–45.

Genderjahn S, Lewin S, Horn F, Schleicher AM, Mangelsdorf K, and Wagner D (2021) Living lithic and sublithic bacterial communities in Namibian drylands. *Microorganisms* 9(2): 235. https://doi.org/10.3390/microorganisms9020235.

Gilbert GK (1877) *Geology of the Henry Mountains*. Washington, DC: U.S. Geological and Geographical Survey 160.

Giorgetti G and Baroni C (2007) High-resolution analysis of silica and sulphate-rich rock varnishes from Victoria land (Antarctica). *European Journal of Mineralogy* 19: 381–389.

Glazovskaya MA (1968) Geochemical landscape and types of geochemical soil sequences. In: *Transactions of 9th International Congress Soil Science, Adelaide IV* 303–311.

Glazovskaya MA (1973) Technogiogeomes—The initial physical geographic objects of landscape geochemical prediction. *Soviet Geography* 14(4): 215–228.

Goldsmith Y, Stein M, and Enzel Y (2014) From dust to varnish: Geochemical constraints on rock varnish formation in the Negev Desert, Israel. *Geochimica et Cosmochimica Acta* 126: 97–111.

Golubic S, Friedmann E, and Schneider J (1981) The lithobiontic ecological niche, with special reference to microorganisms. *Journal of Sedimentary Petrology* 51: 475–478.

Gomez-Heras M, Benavente D, Buergo MA, and Fort R (2004) Soluble salt minerals from pigeon droppings as potential contributors to the decay of stone based cultural heritage. *European Journal of Mineralogy* 16: 505–509.

Goosens D, Mees F, Ranst EV, Tack P, Vincze L, and Poesen J (2015) Rock fragments with dark coatings in slope deposits of the Famenne region, southern Belgium. *Belgeo* 4. https://doi.org/10.4000/belgeo.17625.

Gorbushina AA (2007) Life on the rocks. *Environmental Microbiology* 9: 1613–1631.

Gordon SJ and Dorn RI (2005a) In situ weathering rind erosion. *Geomorphology* 67: 97–113.

Gordon SJ and Dorn RI (2005b) Localized weathering: Implications for theoretical and applied studies. *The Professional Geographer* 57: 28–43.

Goudie AS (1978) Dust storms and their geomorphological implications. *Journal of Arid Environments* 1: 291–310.

Haberland W (1975) Untersuchungen an Krusten, Wustenlacken und Polituren auf Gesteinsoberflachen der nordlichen und mittlerent Saharan (Libyen und Tchad). *Berliner Geographische Abhandlungen* 21: 1–77.

Hall K, Thorn CE, and Sumner A (2012) On the persistence of 'weathering'. *Geomorphology* 149–150: 1–10.

Ha-mung T (1968) The biological nature of iron-manganese crusts of soil-forming rocks in Sakhalin mountain soils. *Microbiology* 36: 621–624.

Harrington CD (1986) Investigation of desert rock varnish on a cobble from a stone burial mound at al-Farrah, al-Jubah Quadrangle, Yemen Arab Republic. In: Overstreet WCAO (ed.) *Geological and Archaeological Reconnaissance in the Yemen Arab Republic, 1985, the Wadi Al-Jubah Archaeological Project*. vol. 4, pp. 41–46. Washington, DC: American Foundation for the Study of Man.

Harrison R and Frink DS (2000) The OCR carbon dating procedure in Australia: New dates from Wilinyjibari Rockshelter, southeaster Kimberley, Western Australia. *Australian Archaeology* 51: 6–15.

Hayden J (1976) Pre-altithermal archaeology in the sierra pinacate, Sonora, Mexico. *American Antiquity* 41: 274–289.

Hetu B, Vansteijn H, and Vandelac P (1994) Flows of frost-coated clasts—A recently discovered scree slope grain-flow type. *Géographie Physique et Quaternaire* 48: 3–22.

Hill CA (1982) Origin of black deposits in caves. *National Speleological Society Bulletin* 44: 15–19.

Hoar K, Nowinski P, Hodge VF, and Cizdziel JV (2011) Rock varnish: A passive forensic tool for monitoring recent air pollution and source identification. *Nuclear Technology* 175: 351–359.

Hodge VF, Farmer DE, Diaz TA, and Orndorff RL (2005) Prompt detection of alpha particles from Po-210: Another clue to the origin of rock varnish? *Journal of Environmental Radioactivity* 78: 331–342.

Hortola P (2005) SEM examination of human erythrocytes in uncoated bloodstains on stone: Use of conventional as environmental-like SEM in a soft biological tissue (and hard inorganic material). *Journal of Microscopy (Oxford)* 218: 94–103.

Howard AD (1994) A detachment-limited model of drainage basin evolution. *Water Resources Research* 30: 2261–2285.

Huelin SR, Longerich HP, Wilton DHC, and Fryer BJ (2006) The determination of trace elements in Fe–Mn oxide coatings on pebbles using LA-ICP-MS. *Journal of Geochemical Exploration* 91: 110–124.

Hungate B, Danin A, Pellerin NB, Stemmler J, Kjellander P, Adams JB, and Staley JT (1987) Characterization of manganese-oxidizing (MnII → MnIV) bacteria from Negev Desert rock varnish: Implications in desert varnish formation. *Canadian Journal of Microbiology* 33: 939–943.

Hunt AG and Wu JQ (2004) Climatic influences on Holocene variations in soil erosion rates on a small hill in the Mojave Desert. *Geomorphology* 58: 263–289.

Huyge D, Watchman A, De Dapper M, and Marchi E (2001) Dating Egypt's oldest 'art': AMS ^{14}C age determinations of rock varnishes covering petroglyphs at El-Hosh (upper Egypt). *Antiquity* 75: 68–72.

Israeli Y, Salhov E, and Emmanuel S (2021) Impact of textural patterns on modeled rock weathering rates and size distribution of weathered grains. *Earth Surface Processes and Landforms* 46: 1177–1187.

Jenne EA (1968) Controls on Mn, Fe, Co, Ni, Cu and Zn concentrations in soils and water: The significant role of hydrous Mn and Fe oxides. In: Gould RF (ed.) *Trace Inorganics in Water*, pp. 337–387. Washington, DC: American Chemical Society.

Jordan DW (1954) The adhesion of dust particles. *British Journal of Applied Physics* 5: S194–S198.

Kendall CGS, Sadd JL, and Alsharhan A (1994) Holocene marine cement coatings on beach-rocks of the Abu-Dhabi coastline (UAE)—Analogs for cement fabrics in ancient limestones. *Carbonates and Evaporites* 9: 119–131.

Kim JG, Lee GH, Lee J, Chon C, Kim TH, and Ha K (2006) Infiltration pattern in a regolith-fractured bedrock profile: Field observations of a dye stain pattern. *Hydrological Processes* 20: 241–250.

Knauss KG and Ku TL (1980) Desert varnish: Potential for age dating via uranium-series isotopes. *Journal of Geology* 88: 95–100.

Konhauser KO, Fyfe WS, Schultze-Lam S, Ferris FG, and Beveridge TJ (1994) Iron phosphate precipitation by epilithic microbial biofilms in Arctic Canada. *Canadian Journal of Earth Sciences* 31: 1320–1324.

Kraft MD, Michalski JR, and Sharp TG (2004) High-silica rock coatings: TES surface-type 2 and chemical weathering on Mars. *35th Lunar and Planetary Science Conference, March 15–19, 2004, League City, Texas, Abstract No. 1936* vol. 35.

Krinsley D (1998) Models of rock varnish formation constrained by high resolution transmission electron microscopy. *Sedimentology* 45: 711–725.

Krinsley DH, Dorn RI, and Tovey NK (1995) Nanometer-scale layering in rock varnish: Implications for genesis and paleoenvironmental interpretation. *Journal of Geology* 103: 106–113.

Krinsley D, Dorn RI, and DiGregorio BE (2009) Astrobiological implications of rock varnish in Tibet. *Astrobiology* 9: 551–562.

Krinsley DH, Dorn RI, DiGregorio BE, Langworthy KA, and Ditto J (2012) Rock varnish in New York: An accelerated snapshot of accretionary processes. *Geomorphology* 138: 339–351.

Krinsley D, Ditto J, Langworthy K, Dorn RI, and Thompson T (2013) Varnish microlaminations: New insights from focused ion beam preparation. *Physical Geography* 34: 159–173.

Krinsley DH, Dorn RI, DiGregorio BE, Razink J, and Fisher R (2017) Mn-Fe enhancing budding bacteria in century-old rock varnish, Erie Canal, New York. *Journal of Geology* 125: 317–336.

Krumbein WE (1969) Über den Einfluss der Mikroflora auf die Exogene Dynamik (Verwitterung und Krustenbildung). *Geologische Rundschau* 58: 333–363.

Krumbein WE (1979) Photolithotrophic and chemoorganotrophic activity of bacteria and algae as related to beachrock formation and degradation (Gulf of Aqaba, Sinai). *Geomicrobiology Journal* 1: 139–203.

Krumbein WE and Jens K (1981) Biogenic rock varnishes of the Negev Desert (Israel): An ecological study of iron and manganese transformation by cyanobacteria and fungi. *Oecologia* 50: 25–38.

Kuhlman KR, Allenbach LB, Ball CL, Fusco WG, La Duc MT, Kuhlman GM, Anderson RC, Stuecker T, Erickson IK, Benardini J, and Crawford RL (2005) Enumeration, isolation, and characterization of ultraviolet (UV-C) resistant bacteria from rock varnish in the Whipple Mountains, California. *Icarus* 174: 585–595.

Kuhlman KR, Fusco WG, La Duc MT, Allenbach LB, Ball CL, Kuhlman GM, Anderson RC, Erickson K, Stuecker T, Benardini J, Strap JL, and Crawford RL (2006a) Diversity of microorganisms within rock varnish in the Whipple Mountains, California. *Applied and Environmental Microbiology* 72: 1708–1715.

Kuhlman KR, McKay CP, Venkat P, La Duc MT, Kulman GM, and Principe E (2006b) Microbial fauna associated with rock varnish at Yungay, Atacama Desert, Chile. *Astrobiology* 6: 153–154.

Kuhlman KR, Venkat P, La Duc MT, Kulman GM, and McKay CP (2008) Evidence of a microbial community associated with rock varnish at Yungay, Atacama Desert, Chile. *Journal of Geophysical Research* 113: G04022. https://doi.org/10.1029/2007JG000677.

Kurtz HD and Netoff DI (2001) Stabilization of friable sandstone surfaces in a desiccating, wind-abraded environment of south-Central Utah by rock surface microorganisms. *Journal of Arid Environments* 48(1): 89–100.

Lacap-Bugler DC, Lee KK, Archer S, Gillman LN, Lau MC, Leuzinger S, Lee CK, Maki T, McKay CP, Perrott JK, and de Los Rios-Murillo A (2017) Global diversity of desert hypolithic cyanobacteria. *Frontiers in Microbiology* 8(867). https://doi.org/10.3389/fmicb.2017.00867.

Langworthy K, Krinsley D, and Dorn RI (2010) High resolution transmission electron microscopy evaluation of silica glaze reveals new textures. *Earth Surface Processes and Landforms* 35: 1615–1620.

Lang-Yona N, Maier S, Macholdt DS, Müller-Germann I, Yordanova P, Rodriguez-Caballero E, Jochum KP, Al-Amri A, Andreae MO, Fröhlich-Nowoisky J, and Weber B (2018) Insights into microbial involvement in desert varnish formation retrieved from metagenomic analysis. *Environmental Microbiology Reports* 10: 264–271.

Lanza NL, Fischer WW, Wiens RC, Grotzinger J, Ollila AM, Cousin A, Anderson RB, Clark BC, Gellert R, Mangold N, and Maurice S (2014a) High manganese concentrations in rocks at Gale crater, Mars. *Geophysical Research Letters* 41: 5755–5763.

Lanza NL, Ollila AM, Cousin A, Hardgrove C, Wiens RC, Mangold N, Nachon M, Fabre C, Bridges N, Johnson J, and Le Mouelic S (2014b) Manganese trends with depth on rock surfaces in gale crater, Mars. *45th Lunar and Planetary Science Conference* vol. 45, 2599.

Lanza NL, Ollila AM, Cousin A, Wiens RC, Clegg S, Mangold N, Bridges N, Cooper D, Schmidt M, Berger J, and Arvidson R (2015) Understanding the signature of rock coatings in laser-induced breakdown spectroscopy data. *Icarus* 249: 62–73.

Larson PH and Dorn RI (2012) Painting Yosemite Valley: A case study of rock coatings encountered at half dome. *Physical Geography* 33: 165–182.

Lavoie KH, Winter AS, Read KJ, Hughes EM, Spilde MN, and Northup DE (2017) Comparison of bacterial communities from lava cave microbial mats to overlying surface soils from lava beds national monument, USA. *PLoS One* 12(2): e0169339. https://doi.org/10.1371/journal.pone.0169339.

Lee MR and Parsons I (1999) Biomechanical and biochemical weathering of lichen-encrusted granite: Textural controls on organic-mineral interactions and deposition of silica-rich layers. *Chemical Geology* 161: 385–397.

Leverington DW and Schindler M (2018) Delineating areas of past environmental degradation near smelters using rock coatings: A case study at Rouyn-Noranda, Quebec. *Scientific Reports* 8: 17364. https://doi.org/10.1038/s41598-018-35742-4.

Li FX, Margetts S, and Fowler I (2001) Use of 'chalk' in rock climbing: Sine quanon or myth? *Journal of Sports Sciences* 19: 427–432.

Li Y, Li Y, Ding H, Lu A, Wang H, Yang X, and Xu X (2017) Mineralogical characteristics of Fe–Mn cutans in yellow brown earth of Wuhan, China. *Journal of Nanoscience and Nanotechnology* 17: 6873–6880.

Li W, Su H, and Pan Y (2019) Research status and prospect of rock varnish. *Geographical Science Research* 8(3). https://doi.org/10.12677/GSER.2019.83028.

Lingappa UF, Yeager CM, Sharma A, Lanza NL, Morales DP, Xie G, Atencio AD, Chadwick GL, Monteverde DR, Magyar JS, and Webb SM (2021) An ecophysiological explanation for manganese enrichment in rock varnish. *Proceedings of the National Academy of Sciences* 118(25): e2025188118. https://www.pnas.org/content/pnas/118/25/e2025188118.full.pdf.

Liu T (2003) Blind testing of rock varnish microstratigraphy as a chronometric indicator: Results on late Quaternary lava flows in the Mojave Desert, California. *Geomorphology* 53: 209–234.

Liu T (2010) VML Dating Lab. http://www.vmldating.com/. Accessed 1 October, 2010.

Liu T (2021) VML Dating Lab. http://www.vmldating.com/. Accessed 31 July.

Liu T and Broecker WS (2000) How fast does rock varnish grow? *Geology* 28: 183–186.

Liu T and Broecker WS (2007) Holocene rock varnish microstratigraphy and its chronometric application in drylands of western USA. *Geomorphology* 84: 1–21.

Liu T and Broecker WS (2008a) Rock varnish evidence for latest Pleistocene millennial-scale wet events in the drylands of western United States. *Geology* 36: 403–406.

Liu T and Broecker WS (2008b) Rock varnish microlamination dating of late quaternary geomorphic features in the drylands of the western USA. *Geomorphology* 93: 501–523.

Liu T and Broecker WS (2013) Millennial-scale varnish microlamination dating of late Pleistocene geomorphic features in the drylands of western USA. *Geomorphology* 187: 38–60.

Liu T, Broecker W, and Stein M (2013) Rock varnish evidence for a younger Dryas wet event in the Dead Sea basin. *Geophysical Research Letters* 40: 2229–2235.

Liu T, Lepre CJ, and Hemming SR (2021) Rock varnish record of the African humid period in the Lake Turkana basin of East Africa. *The Holocene*. https://doi.org/10.1177/09596836211011655.

Loendorf LL (1991) Cation-ratio varnish dating and petroglyph chronology in southeastern Colorado. *Antiquity* 65: 246–255.

Loso MG and Doak DF (2006) The biology behind lichenometric dating curves. *Oecologia* 147: 229–233.

Lozano RP and Rossi C (2012) Exceptional preservation of Mn-oxidizing microbes in cave stromatolites (El Soplao, Spain). *Sedimentary Geology* 255–256: 42–55.

Lu A, Li Y, Ding H, Xu X, Li Y, Ren G, Liang J, Liu Y, Hong H, Chen N, and Chu S (2019) Photoelectric conversion on Earth's surface via widespread Fe- and Mn-mineral coatings. *Proceedings of the National Academy of Sciences* 116: 9741–9746.

Lytle FW, Pingitore NE, Lytle NW, Ferris-Rowley D, and Reheis MC (2002) The possibility of dating petroglyphs from the growth rate of desert varnish. In: *Nevada Archaeological Association Meetings Abstracts*.

Macholdt DS, Herrmann S, Jochum KP, Kilcoyne AD, Laubscher T, Pfisterer JH, Pöhlker C, Schwager B, Weber B, Weigand M, and Domke KF (2017) Black manganese-rich crusts on a gothic cathedral. *Atmospheric Environment* 171: 205–220.

Macholdt DS, Jochum KP, Al-Amri A, and Andreae MO (2019) Rock varnish on petroglyphs from the Hima region, southwestern Saudi Arabia: Chemical composition, growth rates, and tentative ages. *The Holocene* 29: 1377–1396. https://doi.org/10.1177/0959683619846979.

Mantha NM, Schindler M, Murayama M, and Hochella MF (2012) Silica- and sulfate-bearing rock coatings in smelter areas: Products of chemical weathering and atmospheric pollution I. Formation and mineralogical composition. *Geochimica et Cosmochimica Acta* 85: 254–274.

Mantha H, Schindler M, and Hochella MF (2019) Occurrence and formation of incidental metallic Cu and CuS nanoparticles in organic-rich contaminated surface soils in Timmins, Ontario. *Environmental Science: Nano*. https://doi.org/10.1039/C8EN00994E.

Marchant DR, Denton GH, Swisher CC, and Potter N (1996) Late Cenozoic Antarctic paleoclimate reconstructed from volcanic ashes in the dry valleys region of southern Victoria land. *Geological Society of America Bulletin* 108: 181–194.

Marnocha C and Dixon JC (2013) Bacterial communities in Fe/Mn films, sulphate crusts, and aluminium glazes from Swedish Lapland: Implications for astrobiology on Mars. *International Journal of Astrobiology* 12: 345–356.

Marshall RR (1962) Natural radioactivity and the origin of desert varnish. *Transactions of the American Geophysical Union* 43: 446–447.

Marston RA (2003) Editorial note. *Geomorphology* 53: 197.

Martínez-Pabello PU, Sedov S, Solleiro-Rebolledo E, Solé J, Pi-Puig T, Alcántara-Hernández RJ, Lebedeva M, Shishkov V, and Villalobos C (2021) Rock varnish in La Proveedora/Sonora in the context of desert geobiological processes and landscape evolution. *Journal of South American Earth Sciences* 10: 102959. https://doi.org/10.1016/j.jsames.2020.102959.

McAlister JJ, Smith BJ, and Torok A (2006) Element partitioning and potential mobility within surface dusts on buildings in a polluted urban environment, Budapest. *Atmospheric Environment* 40: 6780–6790.

McFadden LD, Ritter JB, and Wells SG (1989) Use of multiparameter relative-age methods for age estimation and correlation of alluvial fan surfaces on a desert piedmont, eastern Mojave Desert. *Quaternary Research* 32: 276–290.

McKeown DA and Post JE (2001) Characterization of manganese oxide mineralogy in rock varnish and dendrites using X-ray absorption spectroscopy. *American Mineralogist* 86: 701–713.

McMaster TJ (2012) Atomic force microscopy of the fungi–mineral interface: Applications in mineral dissolution, weathering and biogeochemistry. *Current Opinion in Biotechnology* 23: 562–569.

Meek N and Dorn RI (2000) *Is mushroom rock a ventifact?* Califonia Geology November/December, 18–20.

Mellor A, Short J, and Kirkby SJ (1997) Tafoni in the El Chorro area, Andalucia, southern Spain. *Earth Surface Processes and Landforms* 22: 817–833.

Mergelov N, Mueller CW, Prater I, Shorkunov I, Dolgikh A, Zazovskaya E, Shishkov V, Krupskaya V, Abrosimov K, Cherkinsky A, and Goryachkin S (2018) Alteration of rocks by endolithic organisms is one of the pathways for the beginning of soils on earth. *Scientific Reports* 8: 3367. https://doi.org/10.1038/s41598-018-21682-6.

Meslier V, Casero MC, Dailey M, Wierzchos J, Ascaso C, Artieda O, McCullough PR, and DiRuggiero J (2018) Fundamental drivers for endolithic microbial community assemblies in the hyperarid Atacama Desert. *Environmental Microbiology* 20: 1765–1781.

Metelka V, Baratouz L, Jessell MW, and Naba S (2015) Visible and infrared properties of unaltered to weathered rocks from Precambrian granite-greenstone terrains of the west African craton. *Journal of African Earth Sciences* 112: 570–585.

Meunier A, Sardini P, Robinet JC, and Pret D (2007) The petrography of weathering processes: Facts and outlooks. *Clay Minerals* 42: 415–435.

Milnes AR, Wright MJ, and Thiry M (1991) Silica accumulations in saprolites and soils in South Australia. In: Nettleton WD (ed.) *Occurrence, Characteristics and Genesis of Carbonate, Gypsum and Silica Acumulations in Soils*. vol. 26, pp. 121–149. Madison: Soil Science Society of America Special Publication.

Minitti ME, Weitz CM, Lane MD, and Bishop JL (2005) Rock coatings from vulcano, a Martian analog environment. *Lunar and Planetary Science* 36: 1835.

Minitti ME, Weitz CM, Lane MD, and Bishop JL (2007) Morphology, chemistry, and spectral properties of Hawaiian rock coatings and implications for Mars. *Journal of Geophysical Research* 112(E05015). https://doi.org/10.1029/2006JE002839.

Molnar P, Anderson RS, and Andersson SP (2007) Tectonics, fracturing of rock, and erosion. *Journal of Geophysical Research. Earth Surface* 112. https://doi.org/10.1029/2005JF000433.

Mottershead DN and Pye K (1994) Tafoni on coastal slopes, South Devon, U.K. *Earth Surface Processes and Landforms* 19: 543–563.

Municchia AC, Bartoli F, Bernardini S, Caneva G, DellaVentura G, Ricci MA, Boun Suy T, and Sodo A (2016) Characterization of an unusual black patina on the Neang Khmau temple (archaeological Khmer area, Cambodia): A multidisciplinary approach. *Journal of Raman Spectroscopy* 47: 1467–1472.

Mustoe GE (2018) Biogenic weathering: Solubilization of iron from minerals by epilithic freshwater algae and cyanobacteria. *Microorganisms* 6(8). https://doi.org/10.3390/microorganisms6010008.

Nakatani T, Sugaya S, Yasui M, Okumura S, and Nakamura M (2021) Amorphous silica coating on flank deposits of the 1783 CE eruption at Asama volcano. *Journal of Volcanology and Geothermal Research* 411: 107149. https://doi.org/10.1016/j.jvolgeores.2020.107149.

NASA (2010) HUalalai Satelllite Images—Aster Volcano Archive. http://ava.jpl.nasa.gov/volcano.asp?vnum=1302-04-. Accessed August 5, 2010.

NIAIST (2005) *Atlas of Eh-pH Diagrams. Intercomparison of Thermodynamic Data Bases*. Geological Survey of Japan Open File Report 419 NIAIST1–287.

Nir I, Barak H, Kramarsky-Winter E, and Kushmaro A (2019) Seasonal diversity of the bacterial communities associated with petroglyphs sites from the Negev Desert, Israel. *Annals of Microbiology* 69(10): 1079–1086.

Northrup DE, Barns SM, Yu LE, Spilde MN, Schelble RT, Dano KE, Crossey LJ, Connolly CA, Boston PJ, Natvig DO, and Dahm CN (2003) Diverse microbial communities inhabiting ferromanganese deposits in Lechuguilla and spider caves. *Environmental Microbiology* 5: 1071–1086.

Northup DE, Snider JR, Spilde MN, Porter ML, van de Kamp JL, Boston PJ, Nyberg AM, and Bargar JR (2010) Diversity of rock varnish bacterial communities from black canyon, New Mexico. *Journal of Geophysical Research* 115(G02007). https://doi.org/10.1029/2009JG001107.

Nowinski P, Hodge VF, Lindley K, and Cizdziel JV (2010) Elemental analysis of desert varnish samples in the vicinity of coal-fired power plants and the Nevada test site using laser ablation ICP-MS. *The Open Chemical and Biomedical Methods Journal* 3: 153–168.

Ntokos D (2021) Age estimation of tectonically exposed surfaces using cation-ratio dating of rock varnish. *Catena* 200. https://doi.org/10.1016/j.catena.2021.105167.

Oguchi CT, Matsukura Y, and Kuchitsu N (2002) Environmental and seasonal influences on the spatial distribution of salt efflorescence and weathering on brick kiln walls. *Transactions of the Japanese Geomorphological Union* 23–32: 335–348.

Otter LM, Macholdt DS, Jochum KP, Stoll B, Weis U, Weber B, Scholz D, Haug GH, Al-Amri AM, and Andreae MO (2020) Geochemical insights into the relationship of rock varnish and adjacent mineral dust fractions. *Chemical Geology* 551: 119775. https://doi.org/10.1016/j.chemgeo.2020.119775.

Palmer E (2002) *Feasibility and Implications of a Rock Coating Catena: Analysis of a Desert Hillslope*. M.A. Thesis (Masters thesis) Tempe: Arizona State University.

Palmer FE, Staley JT, Murray RGE, Counsell T, and Adams JB (1985) Identification of manganese-oxidizing bacteria from desert varnish. *Geomicrobiology Journal* 4: 343–360.

Paradise TR (1997) Sandstone weathering from lichen overgrowth on Red Mountain, Arizona. *Geografiska Annaler. Series A, Physical Geography* 79: 177–184.

Patyk-Kara NG, Gorelikova NV, Plakht J, Nechelyustov GN, and Chizhova IA (1997) Desert varnish as an indicator of the age of quaternary formations (Makhtesh Ramon depression, Central Negev). *Transactions (Doklady) of the Russian Academy of Sciences/Earth Science Sections* 353A: 348–351.

Pedley HM (1990) Classification and environmental models of cool freshwater tufas. *Sedimentary Geology* 68: 143–154.

Pentecost A (1985) Association of cyanobacteria with tufa deposits: Identify, enumeration and nature of the sheath material revealed by histochemistry. *Geomicrobiology Journal* 4: 23–98.

Perel'man AI (1961) Geochemical principles of landscape classification. *Soviet Geography Review and Translation* 11(3): 63–73.

Perel'man AI (1966) *Landscape Geochemistry*. (Translation No. 676, Geological Survey of Canada, 1972) Moscow: Vysshaya Shkola 388.

Perry RS and Adams J (1978) Desert varnish: Evidence of cyclic deposition of manganese. *Nature* 276: 489–491.

Perry RS, Dodsworth J, Staley JT, and Engel MH (2004) *Bacterial Diversity in Desert Varnish Third European Workshop on Exo/Astrobiology, Mars: The Search for Life*. Netherlands: European Space Agency Publications 259–260.

Polynov BB (1937) *The Cycle of Weathering*. [Translated from the Russian by A Muir] New York: Nordemann Publishing 220.

Pope GA and Miranda VC (2016) Weathering of Portuguese megaliths: Evidence for rapid adjustment to new environmental conditions. In: Smith BJ and Turkington A (eds.) *Stone Decay: Its Causes and Controls*, pp. 199–223. Dorset: Shaftesbury.

Potgieter-Vermaak SS, Godol R, Van Grieken R, Potgieter JH, Oujja M, and Catillejo M (2004) Micro-structural characterization of black crust and laser cleaning of building stones by micro-Raman and SEM techniques. *Spectrochimica Acta Part A: Molecular and Biomolecular Spectroscopy* 61: 2460–2467.

Potter RM (1979) *The Tetravalent Manganese Oxides: Clarification of Their Structural Variations and Relationships and Characterization of Their Occurrence in the Terrestrial Weathering Environment as Desert Varnish and Other Manganese Oxides*. Ph.D. Dissertation Thesis Pasadena: California Institute of Technology.

Potter RM and Rossman GR (1977) Desert varnish: The importance of clay minerals. *Science* 196: 1446–1448.

Powers LS, Smith HD, Kilungo AP, Ellis WR Jr., McKay CP, Bonaccorsi R, and Roveda JW (2018) In situ real-time quantification of microbial communities: Applications to cold and dry volcanic habitats. *Global Ecology and Conservation* 16: e00458. https://doi.org/10.1016/j.gecco.2018.e00458.

Raiswell R, Benning LG, Davidson L, Tranter M, and Tulaczyk S (2009) Schwertmannite in wet, acid, and oxic microenvironments beneath polar and polythermal glaciers. *Geology* 37: 431–434.

Roberts AP, Burke H, Pring A, Zhoa J, Gibson CT, Popekla-Filcoff RS, Thredgold J, Bland C, and Corporation MMA (2018) Engravings and rock coatings at Pudjinuk Rockshelter No. 2, South Australia. *Journal of Archaeological Science: Reports* 18: 272–284.

Robinson DA and Williams RBG (1992) Sandstone weathering in the high atlas, Morocco. *Zeitschrift für Geomorphologie* 36: 413–429.

Rossi C, Lozano RP, Isanta N, and Hellstrom J (2010) Manganese stromatolites in caves: El Soplao (Cantabria, Spain). *Geology* 38: 1119–1122.

Rowe MW (2001) Dating by AMS radiocarbon analysis. In: Whitley DS (ed.) *Handbook of Rock Art Research*, pp. 139–166. Walnut Creek: Altamira Press.

Rundel PW (1978) Ecological relationships of desert zone lichens. *Bryologist* 81: 277–293.

Sarmast M, Farpoor MH, and Boroujeni IE (2017) Soil and desert varnish development as indicators of landform evolution in central Iranian deserts. *Catena* 149: 98–109.

Sarmast M, Farpoor MH, Jafari A, and Esfandiarpour Borujeni I (2019) Tracing environmental changes and paleoclimate using the micromorphology of soils and desert varnish in Central Iran. *Desert* 24(2): 331–353.

Schindler M and Dorn RI (2017) *Rock and Mineral Coatings: Records of Climate Change, Pollution, and Life*. McLean, VA: GeoScienceWorld 40.

Schindler M and Singer SM (2017) Mineral surface coatings: Environmental records at the nanoscale. *Elements* 13: 159–164.

Schindler M, Berti D, and Hochella MF (2017) Previously unknown mineral-nanomineral relationships with important environmental consequences: The case of chromium release from dissolving silicate minerals. *American Mineralogist* 102: 2142–2145.

Schlesinger WH (1985) The formation of caliche in soils of the Mojave Desert, California. *Geochimica et Cosmochimica Acta* 49: 57–66.

Sharps MC, Grissom CA, and Vicenzi EP (2020) Nanoscale structure and compositional analysis of manganese oxide coatings on the Smithsonian Castle, Washington, DC. *Chemical Geology* 537. https://doi.org/10.1016/j.chemgeo.2020.119486.

Shiffman P, Zierenberg R, Marks N, Bishop JL, and Dyar MD (2006) Acid-fog deposition at Kilauea volcano: A possible mechanism for the formation of siliceous-sulfate rock coatings on Mars. *Geology* 34: 921–924.

Simionescu B, Alflori M, and Olaru M (2009) Protective coatings based on silsesquioxane nanocomposite films for building limestones. *Construction and Building Materials* 23: 3426–3430.

Smith BJ (1994) Weathering processes and forms. In: Abrahams AD and Parsons AJ (eds.) *Geomorphology of Desert Environments*, pp. 39–63. London: Chapman & Hall.

Smith GA and Turner WG (1975) *Indian Rock art of Southern California With Selected Petroglyph Catalog*. Redlands: San Bernardino County Museum Association 150.

Smith BJ, McAlister JJ, Baptista-Neto JA, and Silva MAM (2007) Post-depositional modification of atmospheric dust on a granite building in Central Rio de Janeiro: Implications for surface induration and subsequent stone decay. *Geological Society, London, Special Publications* 271: 153–166.

Soleilhavoup F (2011) Microformes d'accumulation et d'ablation sur les surfaces desertiques du Sahara. *Geomorphologie: Relief, Processus, Environnement* 2: 173–186.

Somonte C and Baied CA (2013) Minimum surface exposure age of stone quarry workshops: Insights on the first rock-varnish microlamination (VML) dates for northwestern Argentina. *Chungara Revista de Antropologia Chilena* 45: 427–445.

Souza-Egipsy V, Wierzchos J, Sancho C, Belmonte A, and Ascaso C (2004) Role of biological soil crust cover in bioweathering and protection of sandstones in a semi-arid landscape (Torrollones de Gabarda, Huesca, Spain). *Earth Surface Processes and Landforms* 29: 1651–1661.

Spades S and Russ J (2005) GC-MS analysis of lipids in prehistoric rock paints and associated oxalate coatings from the lower Pecos region, Texas. *Archaeometry* 45: 115–126.

Spilde MN, Boston PJ, and Northup DE (2002) Subterranean manganese deposits in caves: Analogies to rock varnish? In: *Geological Society of American Abstracts With Programs*. http://gsa.confex.com/gsa/2002AM/finalprogram/abstract_46060.htm.

Spilde MN, Melim LA, Northup DE, and Boston PJ (2013) Anthropogenic lead as a tracer for rock varnish growth: Implications for rates of formation. *Geology* 41: 263–266.

Steelman KL, Boyd CE, and Allen T (2021) Two independent methods for dating rock art: Age determination of paint and oxalate layers at Eagle Cave, TX. *Journal of Archaeological Science* 126: 105315. https://doi.org/10.1016/j.jas.2020.105315.

Sun T, Levin BDA, Guzman JL, Enders A, Muller DA, Angenent LT, and Lehmann J (2017) Rapid electron transfer by the carbon matrix in natural pyrogenic carbon. *Nature Communications* 8: 14873. https://doi.org/10.1038/ncomms14873.

Suzuki T (2002) Rock control in geomorphological processes: Research history in Japan and perspective. *Transactions of the Japanese Geomorphological Union* 23(2): 161–199.

Taylor-George S, Palmer FE, Staley JT, Borns DJ, Curtiss B, and Adams JB (1983) Fungi and bacteria involved in desert varnish formation. *Microbial Ecology* 9: 227–245.

Thiagarajan N and Lee CA (2004) Trace-element evidence for the origin of desert varnish by direct aqueous atmospheric deposition. *Earth and Planetary Science Letters* 224: 131–141.

Vázquez-Ortega A and Fein JB (2017) Thermodynamic modeling of Mn (II) adsorption onto manganese oxidizing bacteria. *Chemical Geology* 464: 147–154.

Vergès-Belmin, Pichot C, and Orial G (1993) Elimination de croûtes noires sur marbre et craie: À quel niveau arrêter le nettoyage? In: Thiel M-J (ed.) *Conservation of Stone and Other Materials*, pp. 535–541. London: E & FN Spon.

Viles HA (1995) Ecological perspectives on rock surface weathering: Towards a conceptual model. *Geomorphology* 13: 21–35.

Viles HA (2001) Scale issues in weathering studies. *Geomorphology* 41: 61–72.

Viles HA and Goudie AS (1990) Tufas, travertines and allied carbonate deposits. *Progress in Physical Geography* 14: 19–41.

Viles HA and Goudie AS (2004) Biofilms and case hardening on sandstones from Al-Quawayra, Jordan. *Earth Surface Processes and Landforms* 29: 1473–1485.

Villa N, Dorn RI, and Clark J (1995) Fine material in rock fractures: Aeolian dust or weathering? In: Tchakerian V (ed.) *Desert Aeolian Processes*, pp. 219–231. London: Chapman & Hall.

von Humboldt A (1812) *Personal Narrative of Travels to the Equinoctial Regions of America During the Years 1799–1804 by Alexander von Humboldt and Aime Bonpland*. Written in French by Alexander von Humboldt Vol. II (Translated and Edited by T Ross in 1907) London: George Bell & Sons 521.

Wadsten T and Moberg R (1985) Calcium oxalate hydrates on the surface of lichens. *The Lichenologist* 17: 239–245.

Wang X, Zeng L, Wiens M, Scholoßmacher U, Jochum KP, Schröder HC, and Müller WEG (2011) Evidence for a biogenic, microorganismal origin of rock varnish from the Gangdese Belt of Tibet. *Micron* 42: 401–411.

Wannier MM, de Urreiztieta M, Wenk HR, Stan CV, Tamura N, and Yue B (2019) Fallout melt debris and aerodynamically-shaped glasses in beach sands of Hiroshima Bay, Japan. *Anthropocene* 25: 100196. https://doi.org/10.1016/j.ancene.2019.10 0196.

Watchman A (1997) Differences of interpretation for Foz Côa dating results. *National Pictographic Society Newsletter* 8(1): 7.

Watchman A (2000) A review of the history of dating rock varnishes. *Earth-Science Reviews* 49: 261–277.

Watchman A (2002) A reply to Whitley and Simon. *INORA* 34: 11–12.

Watchman A, David B, McNiven I, and Flood J (2000) Microarchaeology of engraved and painted rock surface crusts at Yiwaralarlay (the lightning brothers site), Northern Territory, Australia. *Journal of Archaeological Science* 27: 315–325.

Wayne DM, Diaz TA, Fairhurst RJ, Orndorff RL, and Pete DV (2006) Direct major-and trace-element analyses of rock varnish by high resolution laser ablation inductively-coupled plasma mass spectrometry (LA-ICPMS). *Applied Geochemistry* 21: 1410–1431.

Weaver CE (1978) Mn-Fe coatings on saprolite fracture surfaces. *Journal of Sedimentary Petrology* 48: 595–610.

Wen H, Xu W, Li Y, You Y, and Luo X (2020) Siliceous-sulphate rock coatings at Zhenzhu spring, Tengchong, China: The integrated product of acid-fog deposition, spring water capillary action, and dissolution. *Geological Magazine* 157(2): 201–212.

White WB, Vito C, and Scheetz BE (2009) The mineralogy and trace element chemistry of blcak manganese oxide deposits from caves. *Journal of Cave and Karst Studies* 71: 136–143.

Whitley DS and Annegarn HJ (1994) Cation-ratio dating of rock engravings from Klipfontein, Northern Cape Province, South Africa. In: Dowson TA and Lewis-Williams JD (eds.) *Contested Images: Diversity in Southern African Rock Art Research*, pp. 189–197. Johannesburg: University of Witwatersrand Press.

Whitley DS and Simon JM (2002a) Recent AMS radiocarbon rock engraving dates. *INORA* 32: 11–16.

Whitley DS and Simon JM (2002b) Reply to Huyge and Watchman. *INORA* 34: 12–21.

Whitley DS, Simon JM, and Dorn RI (1999) Vision quest in the Coso range. *American Indian Rock Art* 25: 1–31.

Wieler N, Ginat H, Gillor O, and Angel R (2019) The origin and role of biological rock crusts in rocky desert weathering. *Biogeosciences* 16: 1133–1145.

Wieler N, Erickson Gini T, Gillor O, and Angel R (2021) Microbial and geo-archaeological records reveal the growth rate, origin and composition of desert rock surface communities. *Biogeosciences* 18(11): 3331–3342.

Xu H, Chen T, and Konishi H (2010) HRTEM investigation of trilling todorokite and nano-phase Mn-oxides in manganese dendrites. *American Mineralogist* 95: 556–562.

Xu X, Li Y, Li Y, Lu A, Qiao R, Liu K, Ding H, and Wang C (2019) Characteristics of desert varnish from nanometer to micrometer scale: A photo-oxidation model on its formation. *Chemical Geology*. https://doi.org/10.1016/j.chemgeo.2019.05.016.

Yeager C, Lanza N, Marti-Arbona R, Tashima M, Lingappa U, and Fischer W (2019) *Terrestrial Rock Varnish: Implications for Biosignatures on Mars*. LPI Contribution No 2108, id 5060.

Yoshikawa K, Okura Y, Autier V, and Ishimaru S (2006) Secondary calcite crystallization and oxidation processes of granite near the summit of Mt. McKinley, Alaska. *Geomorhpologie: Relief, Processus, Environnement* 3: 197–204.

Yu C, Drake H, Mathurin FA, and Åström ME (2017) Cerium sequestration and accumulation in fractured crystalline bedrock: The role of Mn-Fe (hydr-) oxides and clay minerals. *Geochimica et Cosmochimica Acta* 199: 370–389.

Zerboni A (2008) Holocene rock varnish on the Messak plateau (Libyan Sahara): Chronology of weathering processes. *Geomorphology* 102: 640–651.

Zhang Y, Liu T, and Li S (1990) Establishment of a cation-leaching curve of rock varnish and its application to the boundary region of Gansu and Xinjiang, western China. *Seismology and Geology (Beijing)* 12: 251–261.

Zorin ZM, Churaev N, Esipova N, Sergeeva I, Sobolev V, and Gasanov E (1992) Influence of cationic surfactant on the surface charge of silica and on the stability of acqueous wetting films. *Journal of Colloid and Interface Science* 152: 170–182.